A Review of Laser-Plasma Acceleration of Ions

Andrea Macchi

CNR/INFM/polyLAB, Pisa
Dipartimento di Fisica "Enrico Fermi", Università di Pisa
Pisa, Italy

CLPU, Universidad de Salamanca,
January 10, 2010

Seminario de Optica

A Study of X-ray Generation and Transport in Laser-Irradiated Solid Targets

Andrea Macchi

Scuola Normale Superiore, e Istituto di Fisica Atomica e Molecolare - CNR,

Pisa, Italia

Abstract.- The plasmas produced by interaction of intense laser pulses with solid targets are bright X-ray sources for a number of applications. In order to optimize the performance of these sources, a broad study is currently in progress worldwide. A review of the basic principles of X-ray generation in laser-produced plasmas and an experimental study of the X-ray emission from laser-irradiated Aluminium targets in the nanosecond regime will be presented. This may supply a novel, debris-free X-ray source.

Jueves, 22 de febrero de 1996, a las 17:00 horas, en la supuesta hemeroteca del edificio de Físicas.

Outline

- The “new era” of laser acceleration of ions (mainly protons):
  their discovery and (foreseen) applications
- Target Normal Sheath Acceleration (TNSA)
  - Theory (plasma expansion model)
  - Experimental evidence
  - Review of experimental results and progress
- Radiation Pressure Acceleration (RPA)
  - Theory (role of circular polarization)
  - Preliminary experimental indications

Main contributors to original work presented

Francesco Ceccherini, Fulvio Cornolti,
Sara Tuveri, Silvia Veghini,
Francesco Pegoraro

*Dipartimento di Fisica "Enrico Fermi",
Università di Pisa and CNISM, Pisa*

Tatiana V. Liseykina

*Institute of Computer Technologies,
SD-RAS, Novosibirsk, Russia and
MPI-K, Heidelberg, Germany*

Satyabrata Kar, Lorenzo Romagnani,
Marco Borghesi

*School of Mathematics and Physics,
Queen's University, Belfast, UK*

The discovery of MeV proton emission in superintense interaction with *metallic* targets

Reported in 2000
by three experimental groups

[Clark et al, PRL **84**, 670 (2000);
Maksimchuk et al, *ibid.*, 4108;
Snavely et al, PRL **85**, 2945 (2000) (*)]

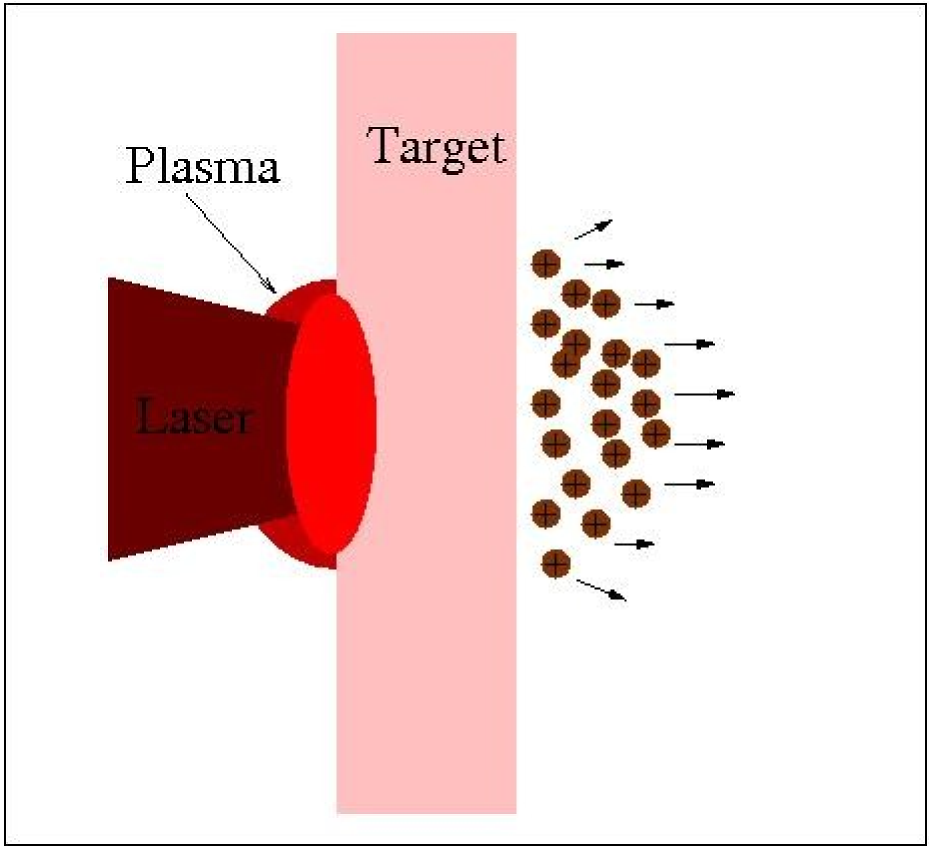

Remarkable properties of the proton beam:

- **high number** (up to 10^{14})
- **good collimation**
- **ultra-low emittance** (4×10^{-3} mm mrad)
- maximum energy and efficiency observed (*):
  58 MeV , **12% of laser energy**
  @ I=3 x 10^{20} W/cm^2

The discovery of MeV proton emission in superintense interaction with *metallic* targets

Reported in 2000
by three experimental groups

[Clark et al, PRL **84**, 670 (2000);
Maksimchuk et al, *ibid.*, 4108;
Snavely et al, PRL **85**, 2945 (2000) (*)]

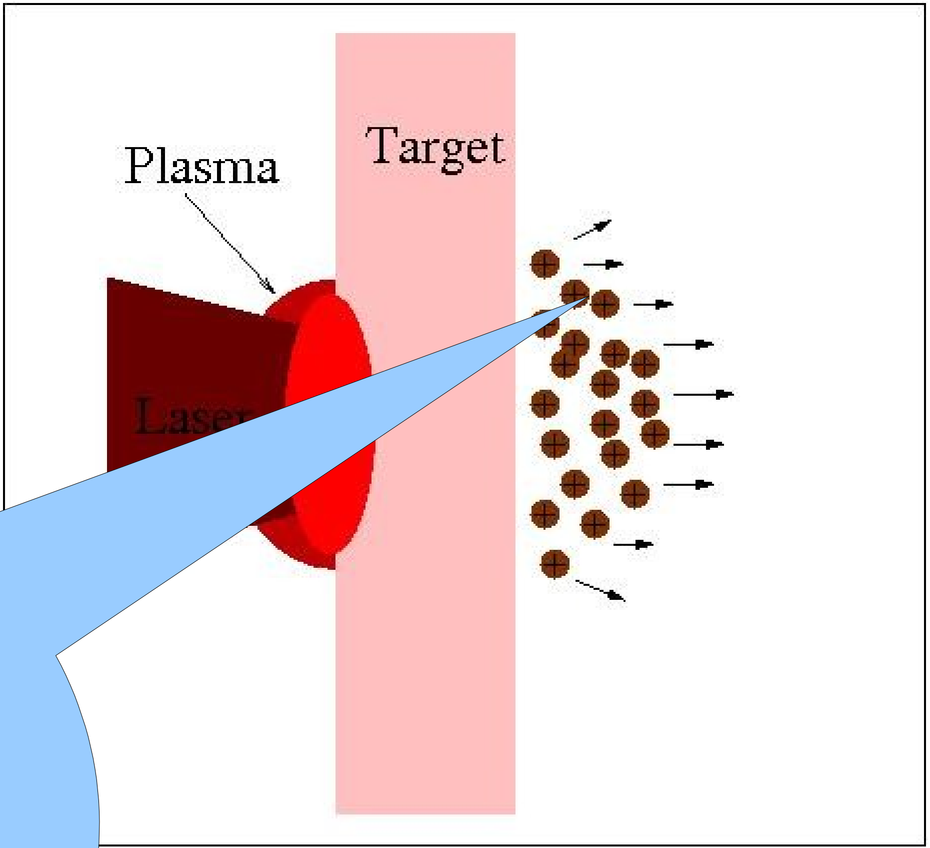

Question: why *protons* from *metallic* targets?

(up to 10^{14})
ation
Remar... **mittance** (4×10^{-3} mm mrad)
of the p... energy and efficiency
...ed (*):
...s MeV , **12% of laser energy**
@ $I=3 \times 10^{20}$ W/cm^2

The discovery of MeV proton emission in superintense interaction with *metallic* targets

Reported in 2000
by three experimental groups

[Clark et al, PRL **84**, 670 (2000);
Maksimchuk et al, *ibid.*, 4108;
Snavely et al, PRL **85**, 2945 (2000) (*)]

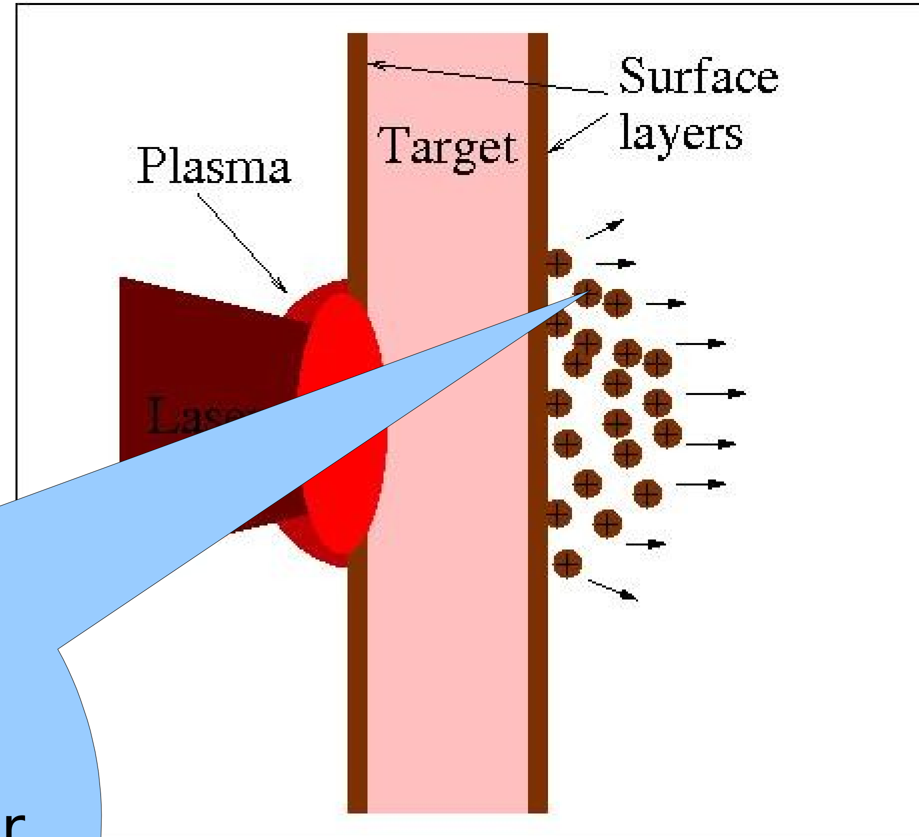

Question: why *protons* from *metallic* targets?

Answer: presence of a layer of hydrocarbon or water impurities on the target surface

(up to 10^{14})
ation
Remar... mittance (4×10^{-3} mm mrad)
of the p... energy and efficiency
...ed (*):
...s MeV , **12% of laser energy**
@ I=3 x 10^{20} W/cm^2

The discovery of MeV proton emission in superintense interaction with *metallic* targets

Reported in 2000
by three experimental groups

[Clark et al, PRL **84**, 670 (2000);
Maksimchuk et al, *ibid.*, 4108;
Snavely et al, PRL **85**, 2945 (2000) (*)]

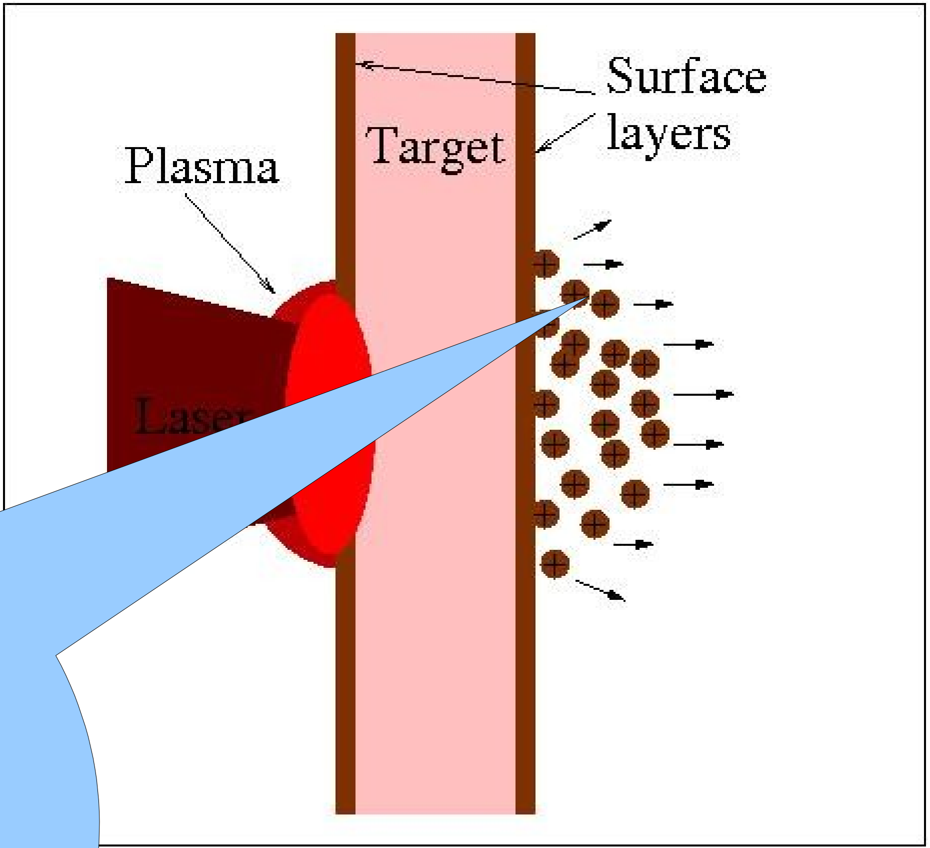

More debated question: are protons coming from the *front* or from the *rear* side?

i.e. *what is the acceleration mechanism*?

(up to 10^{14})
ation
Remar... **mittance** (4×10^{-3} mm mrad)
of the p... energy and efficiency
...ed (*):
...MeV , **12% of laser energy**
@ $I = 3 \times 10^{20}$ W/cm^2

MeV protons (ions) are appealing for applications requiring localized energy deposition in matter

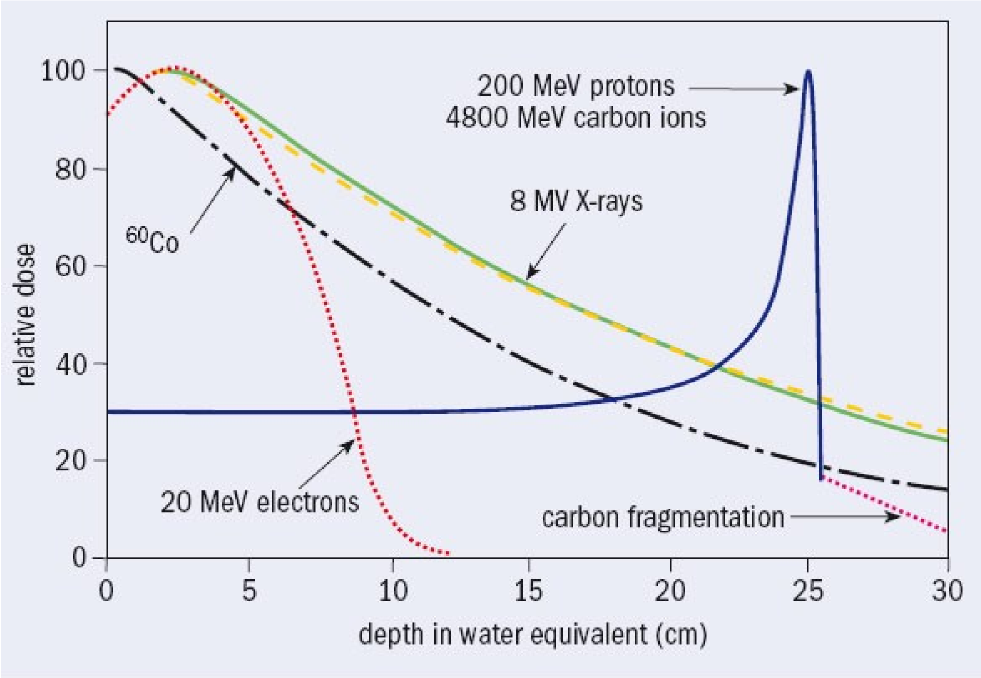

Sharp spatial maximum of deposited energy (Bragg peak)

Peak location depends on energy

[U. Amaldi & G. Kraft, Rep. Prog. Phys. **68**, 1861 (2005)]

MeV protons (ions) are appealing for applications requiring localized energy deposition in matter

Medical Applications

ONCOLOGICAL HADRONTHERAPY

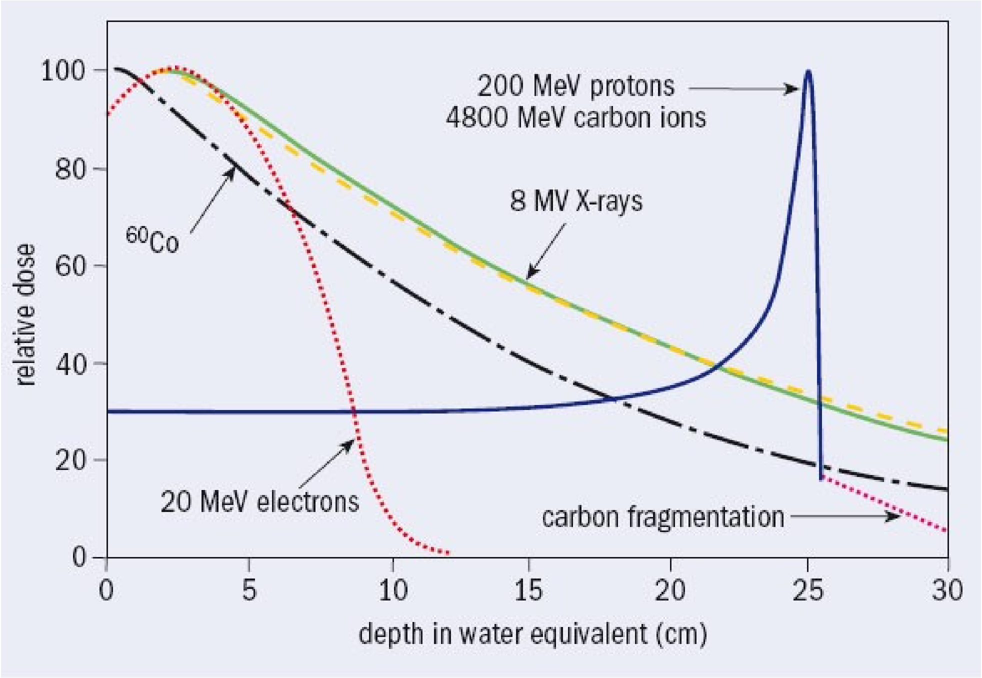

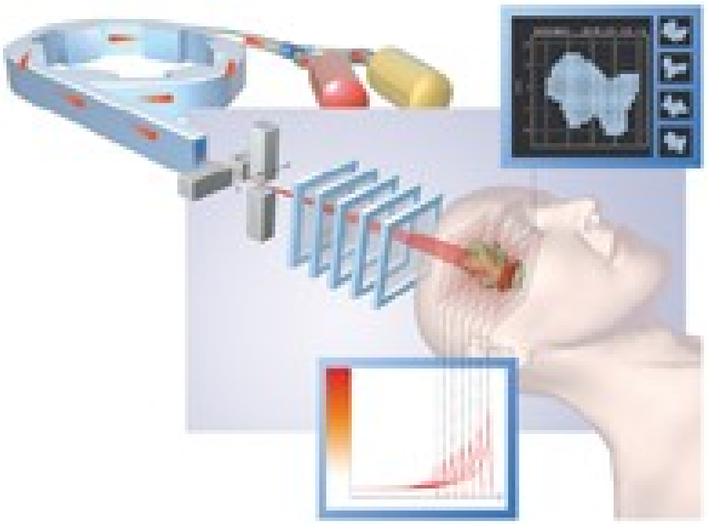

If feasible with table-top, high repetition lasers,
cost might be reduced with respect to an accelerator facility
(***CAUTION***: see Linz & Alonso, PRSTAB **10** (2007) 094801)

Other foreseen application in medicine:
isotope production (e.g. for Proton Emission Tomography)

MeV protons (ions) are appealing for applications requiring localized energy deposition in matter

Inertial **C**onfinement nuclear **F**usion

FAST IGNITION

Protons can be used to create a "spark" in a pre-compressed ICF capsule achieving isochoric burn and high energy gain

[Roth et al, Phys. Rev. Lett. **86** (2001) 436;
Atzeni et al, Nuclear Fusion **42** (2002) L1;
Macchi et al, Nuclear Fusion **43** (2003) 362]

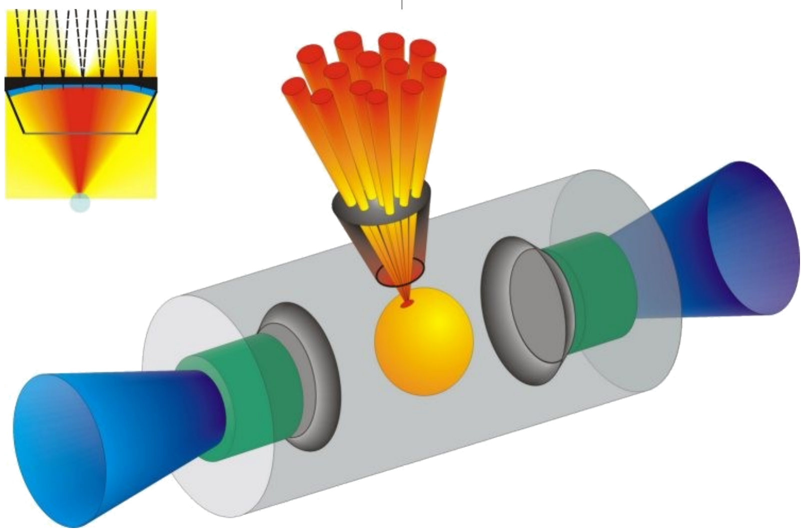

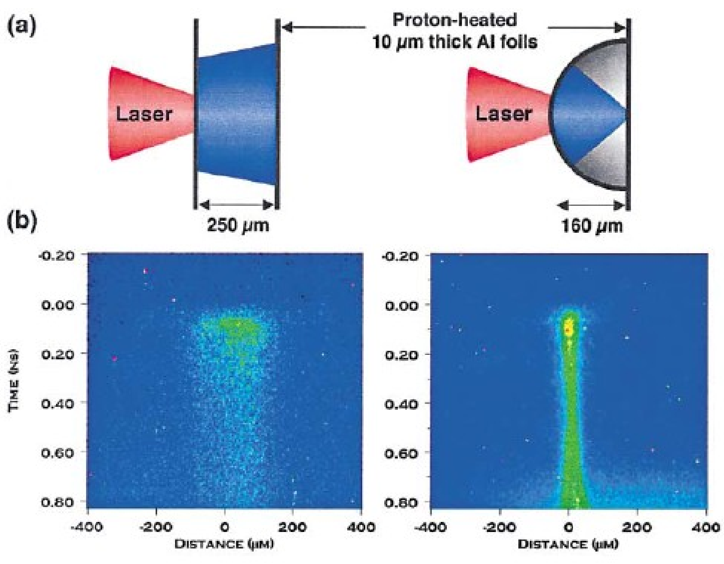

Geometrical focusing of laser-accelerated protons and localized isochoric heating has been demonstrated

[Patel et al, Phys. Rev. Lett. **91** (2003) 125004]

Fast ions seen in PIC simulations suggest several possible mechanisms of ion acceleration

1D PIC simulation

$I = 3.5 \times 10^{20}$ W/cm^2 ,

$n_e = 10^{22}$ cm^{-3}

PIC (Particle-In-Cell):
solves kinetic equations
for ions and electrons
+ Maxwell's equations for
laser and plasma fields

“Idealized” conditions:

- ideal, collisionless plasma

- slab with step-like
  density profile

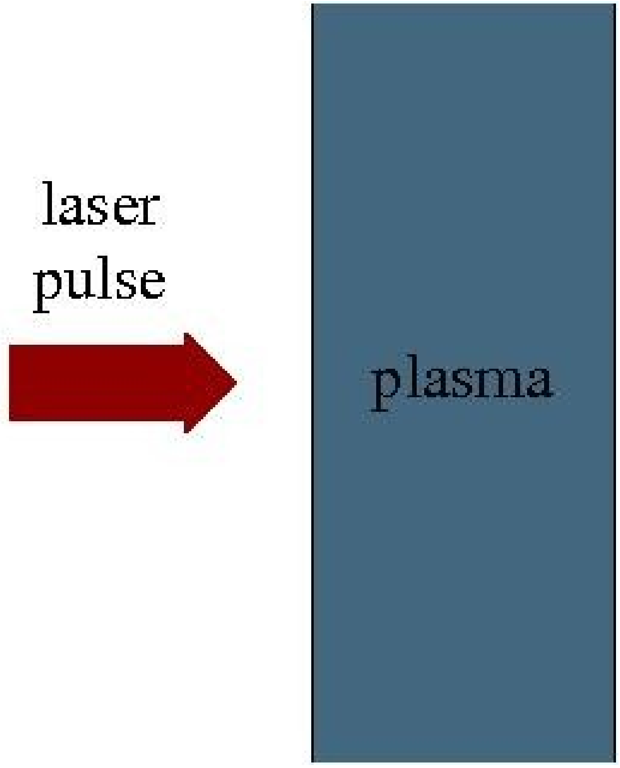

Fast ions seen in PIC simulations suggest several possible mechanisms of ion acceleration

1D PIC simulation

$I = 3.5 \times 10^{20}$ W/cm^2,

$n_e = 10^{22}$ cm^{-3}

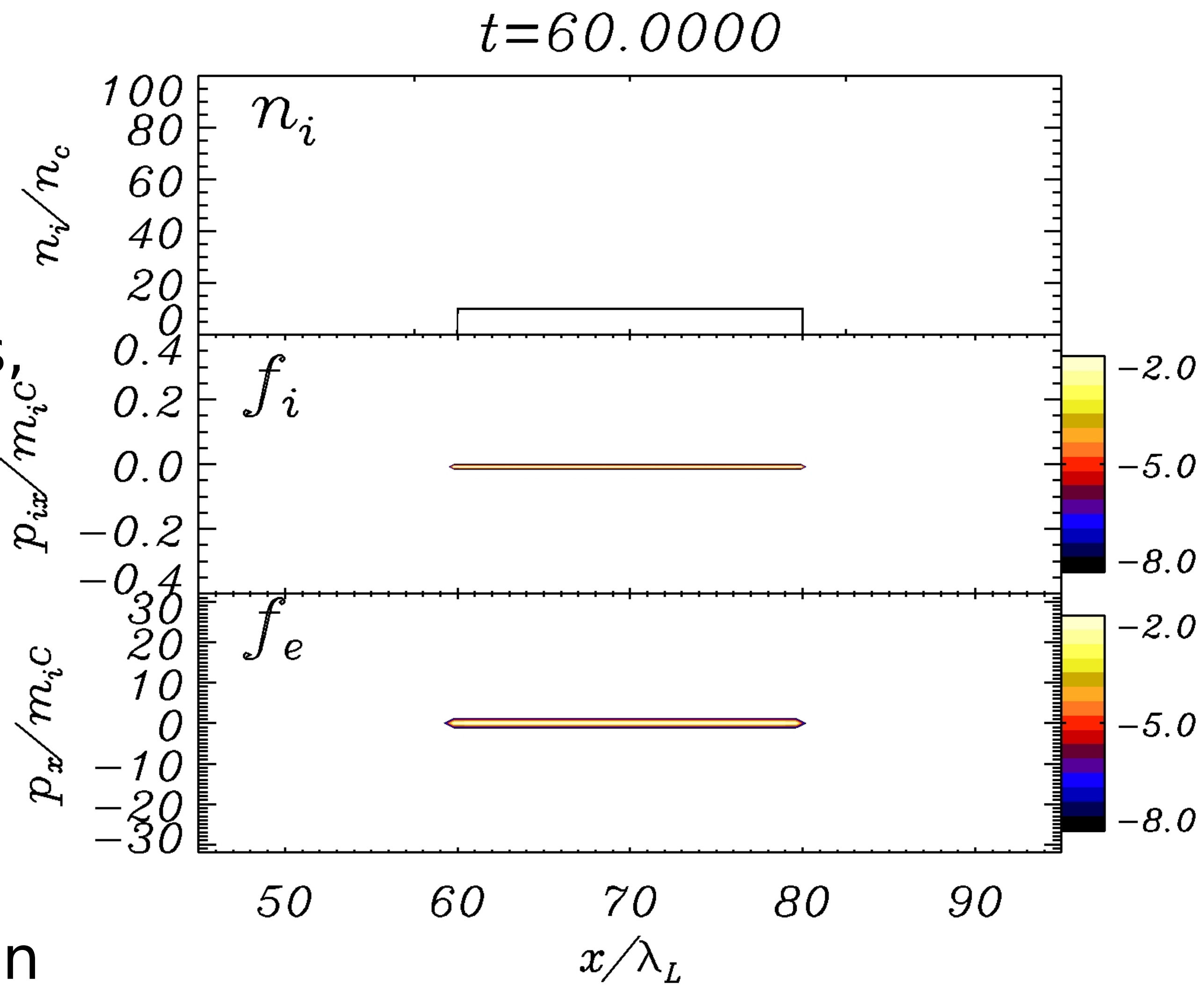

Three ion populations, accelerated

- from rear side in forward direction
- from front side in forward direction
- from front side in backward direction

Which is the dominant "channel" for given conditions?

Fast ions seen in PIC simulations suggest several possible mechanisms of ion acceleration

1D PIC simulation

I=3.5×10^{20}W/cm^2,

n_e=10^{22}cm^{-3}

Three ion populations, accelerated

- from rear side
  in forward direction

- from front side
  in forward direction

- from front side
  in backward direction

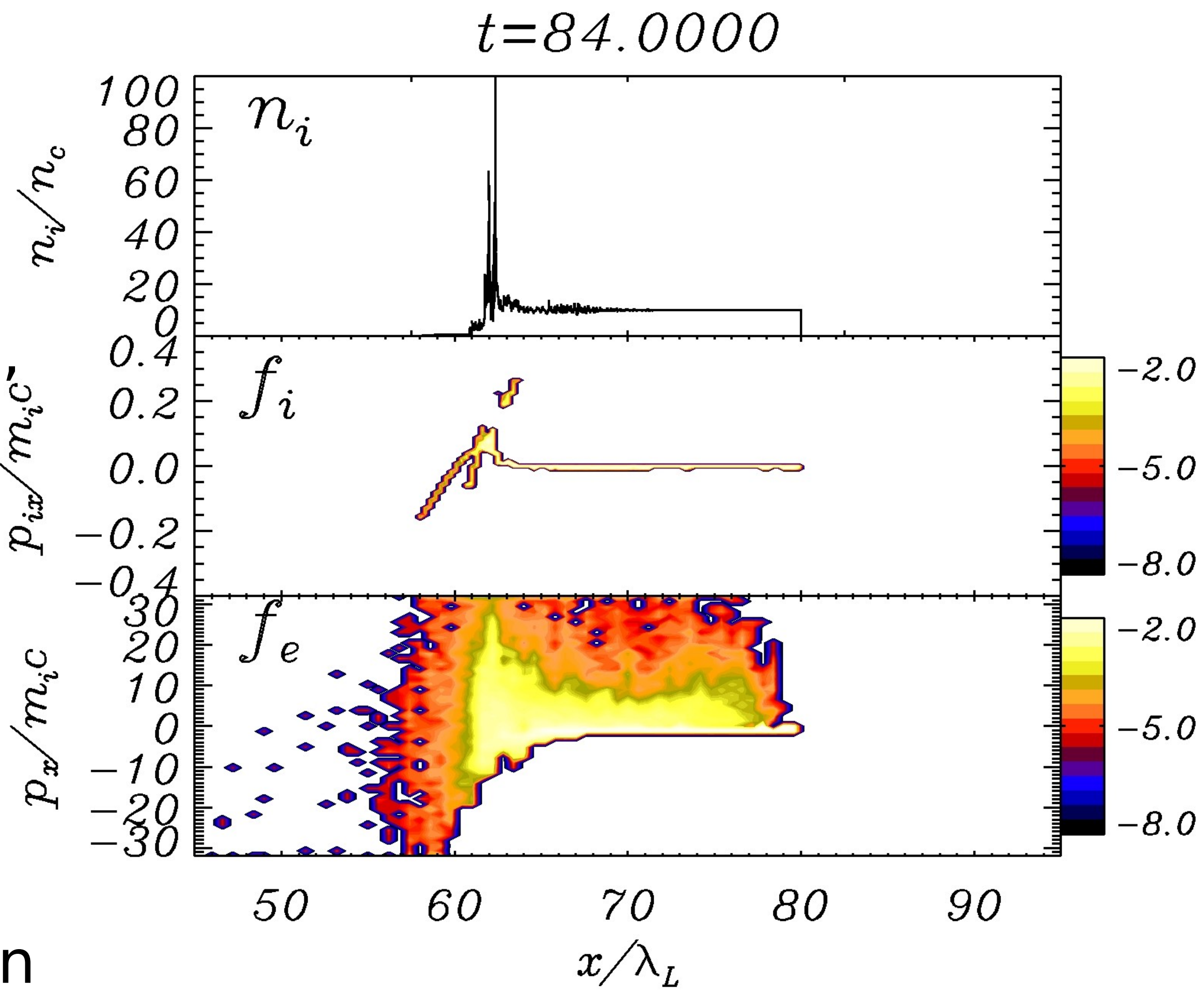

Which is the dominant “channel” for given conditions?

Fast ions seen in PIC simulations suggest several possible mechanisms of ion acceleration

1D PIC simulation

$I = 3.5 \times 10^{20}$ W/cm^2,

$n_e = 10^{22}$ cm^{-3}

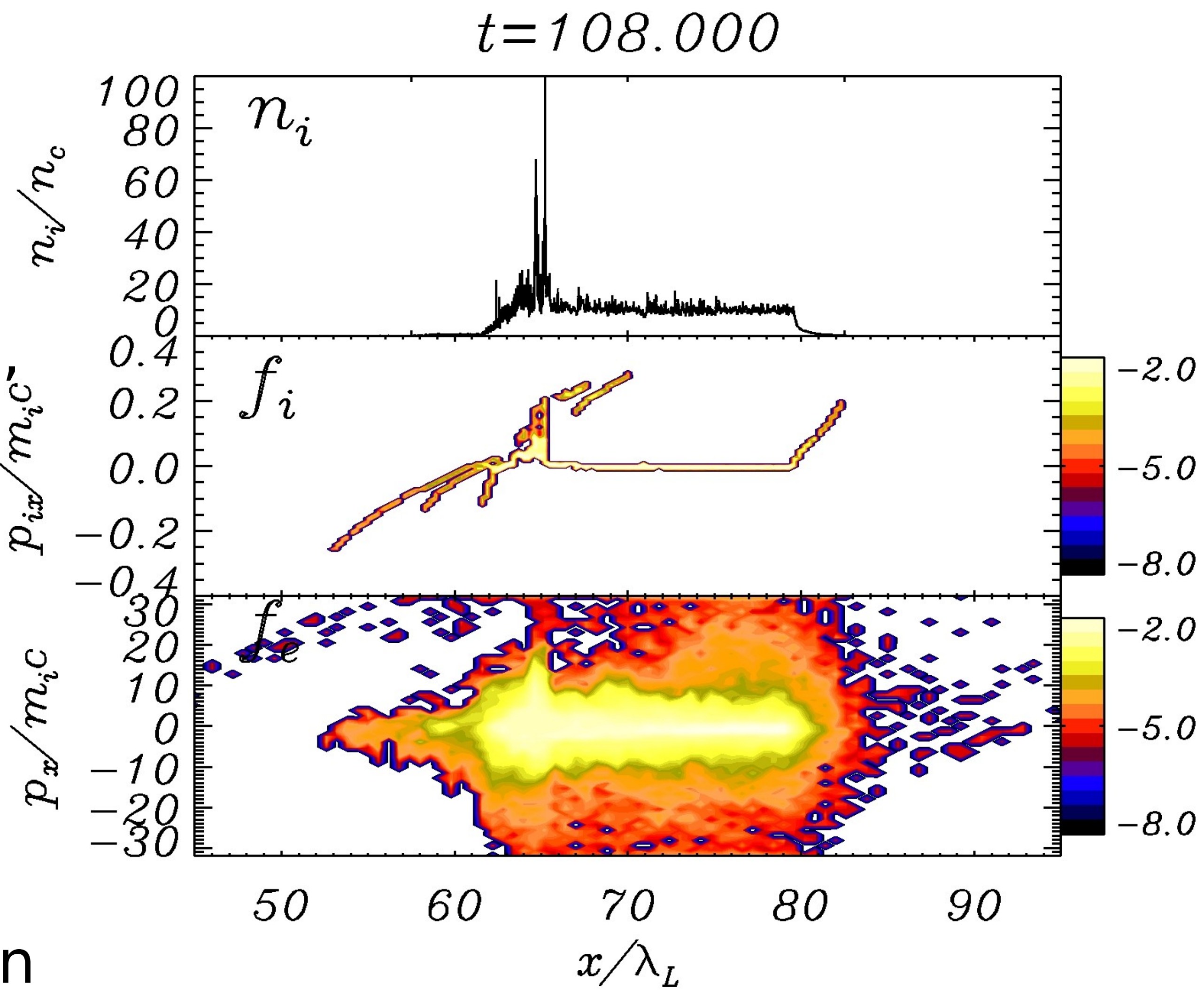

Three ion populations, accelerated

- from rear side in forward direction

- from front side in forward direction

- from front side in backward direction

Which is the dominant “channel” for given conditions?

Fast ions seen in PIC simulations suggest several possible mechanisms of ion acceleration

1D PIC simulation

$I = 3.5\times10^{20}\,\mathrm{W/cm^2}$,

$n_e = 10^{22}\,\mathrm{cm^{-3}}$

Three ion populations, accelerated

- from rear side in forward direction
- from front side in forward direction
- from front side in backward direction

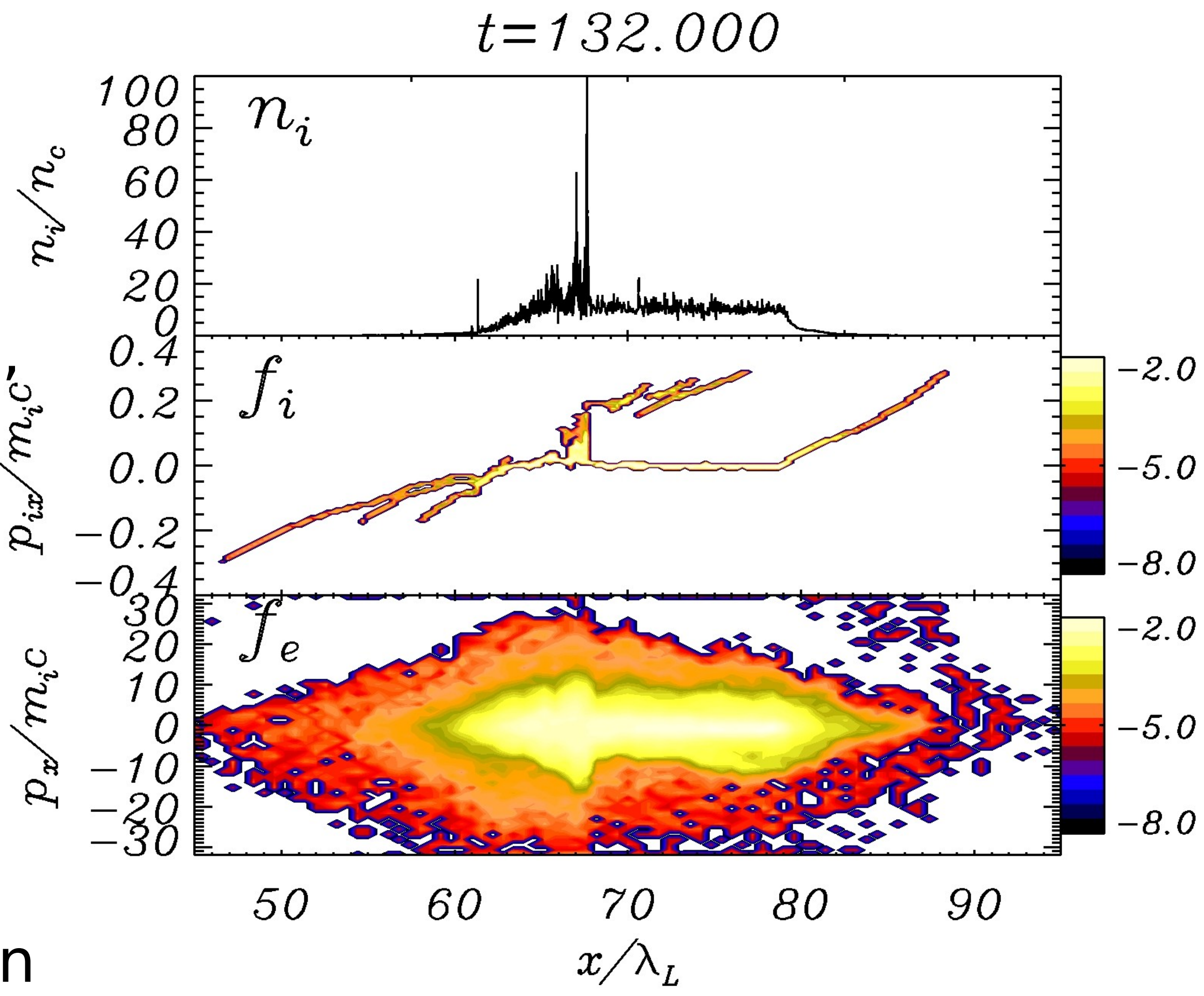

Which is the dominant “channel” for given conditions?

Fast ions seen in PIC simulations suggest several possible mechanisms of ion acceleration

1D PIC simulation
$I=3.5\times10^{20}\,\mathrm{W/cm^2}$,
$n_e=10^{22}\,\mathrm{cm^{-3}}$

Three ion populations, accelerated

- from rear side
  in forward direction

- from front side
  in forward direction

- from front side
  in backward direction

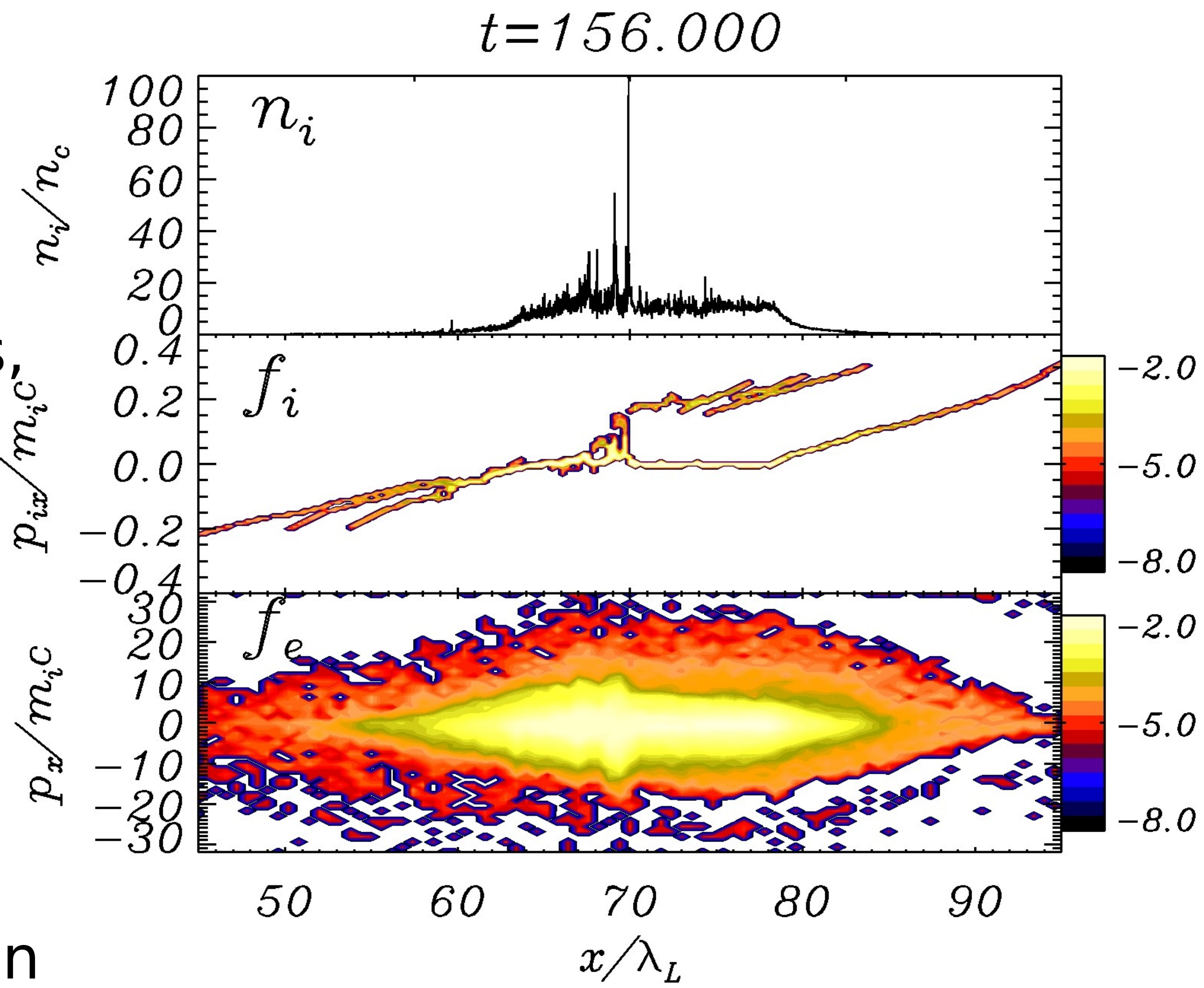

Which is the dominant "channel" for given conditions?

Fast ions seen in PIC simulations suggest several possible mechanisms of ion acceleration

1D PIC simulation

$I=3.5\times10^{20}$ W/cm^2,

$n_e=10^{22}$ cm^{-3}

Three ion populations, accelerated

- from rear side in forward direction
- from front side in forward direction
- from front side in backward direction

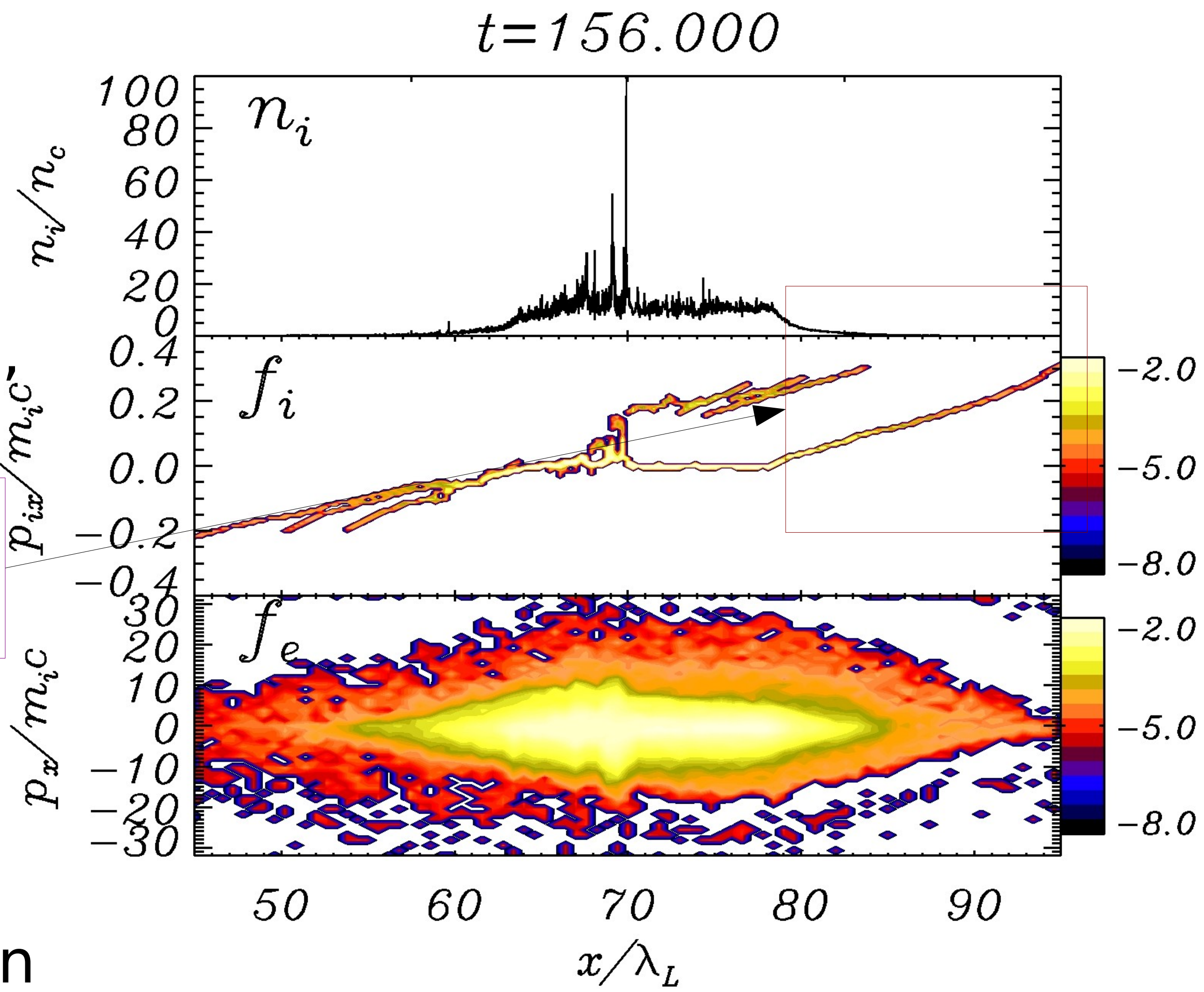

Which is the dominant “channel” for given conditions?

Fast ions seen in PIC simulations suggest several possible mechanisms of ion acceleration

1D PIC simulation
$I = 3.5 \times 10^{20}$ W/cm^2,
$n_e = 10^{22}$ cm^{-3}

Three ion populations, accelerated

- from rear side in forward direction

- from front side in forward direction

- from front side in backward direction

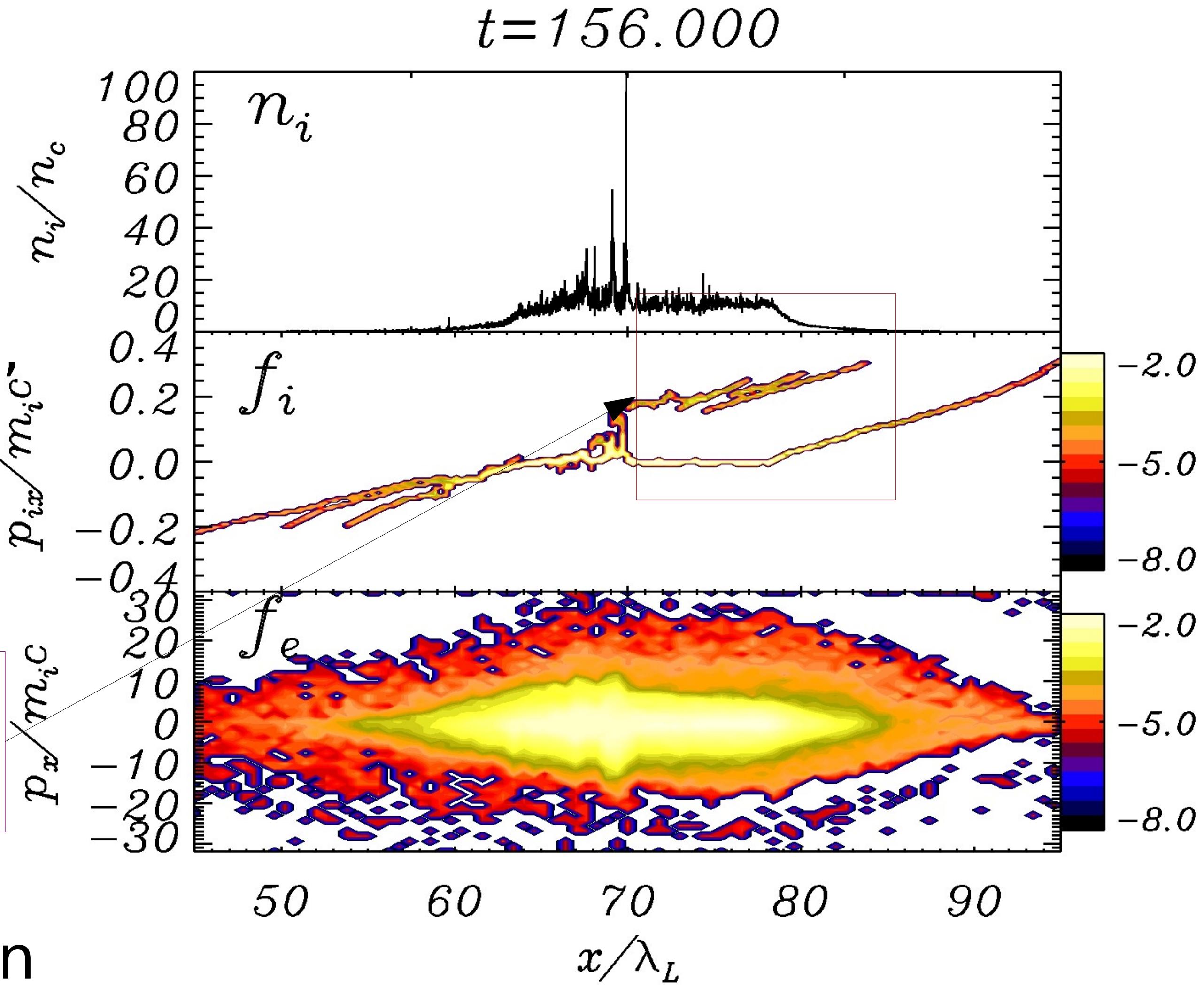

Which is the dominant “channel” for given conditions?

Fast ions seen in PIC simulations suggest several possible mechanisms of ion acceleration

1D PIC simulation

$I = 3.5\times10^{20}$ W/cm^2,

$n_e = 10^{22}$ cm^{-3}

Three ion populations, accelerated

- from rear side in forward direction
- from front side in forward direction
- from front side in backward direction

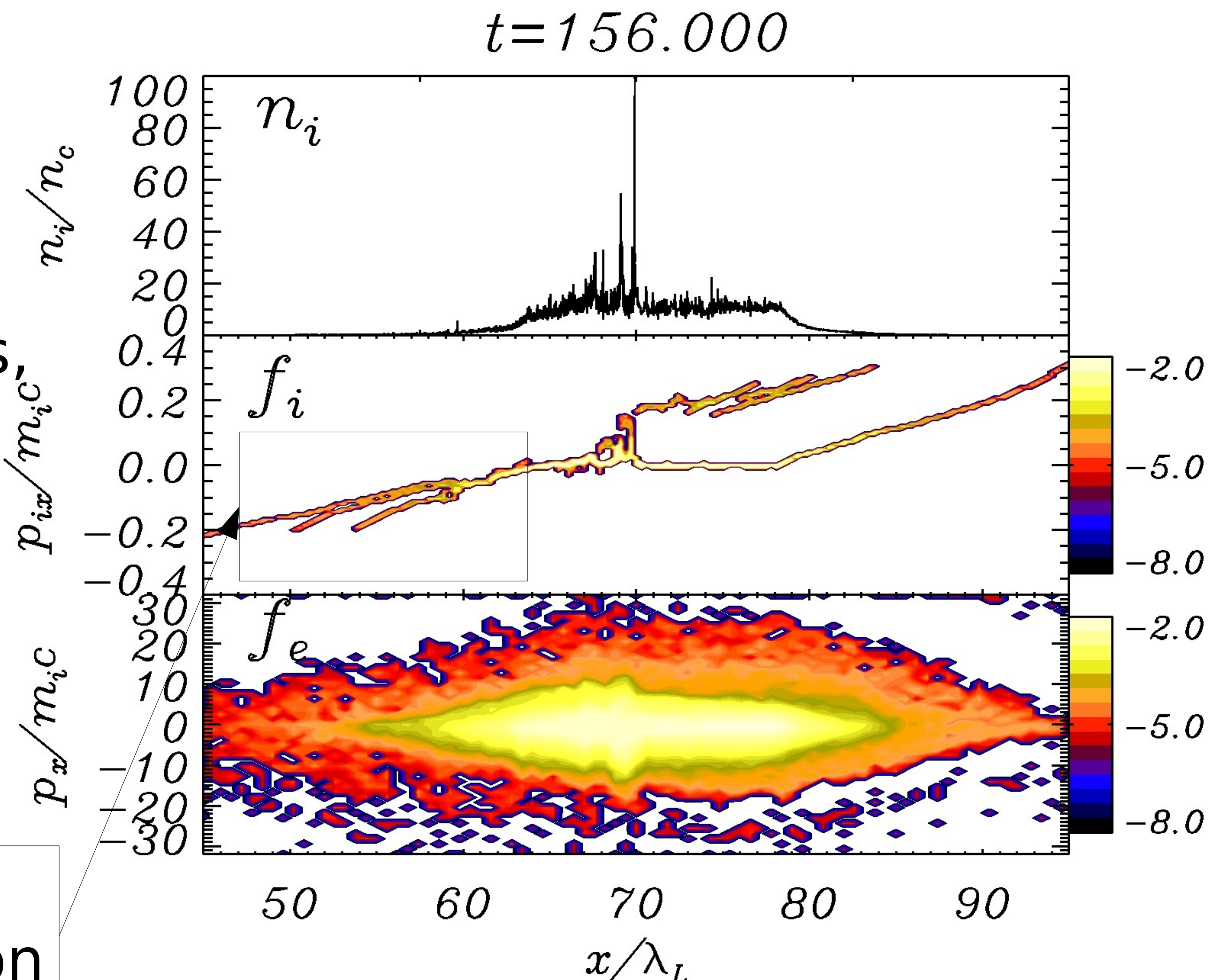

Which is the dominant “channel” for given conditions?

Fast ions seen in PIC simulations suggest several possible mechanisms of ion acceleration

1D PIC simulation

$I = 3.5 \times 10^{20}\,\mathrm{W/cm^2}$,

$n_e = 10^{22}\,\mathrm{cm^{-3}}$

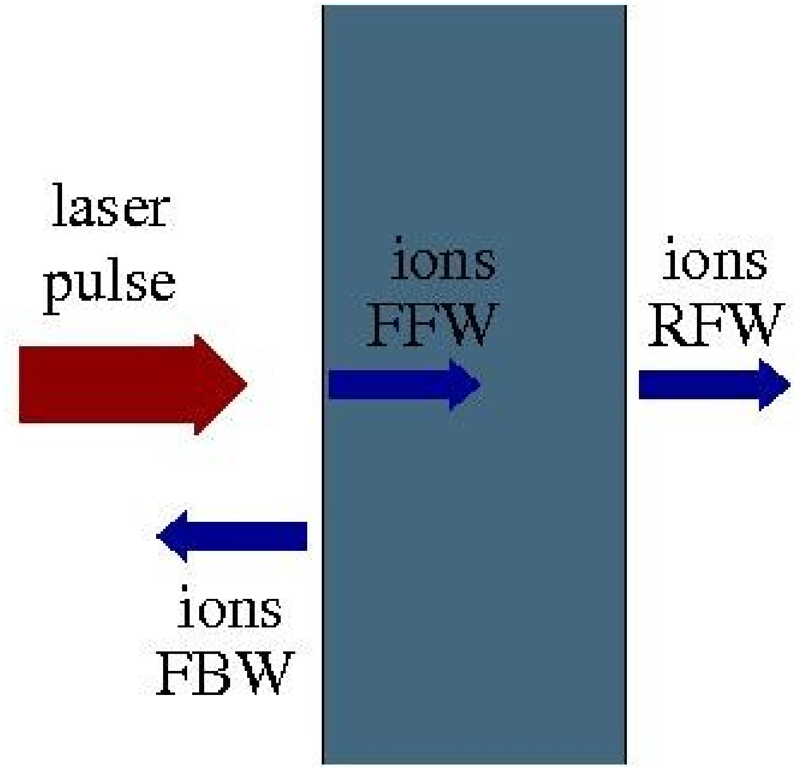

Three ion populations, accelerated

- from rear side
  in forward direction

- from front side
  in forward direction

- from front side
  in backward direction

Which is the dominant “channel” for given conditions?

The "front vs rear side" debate

Clark et al: "It is likely that the protons originate from the front surface of the target and are bent by large magnetic fields which exist in the target interior."

Maksimchuk et al: "The protons [...] appear to originate from impurities on the front side of the target [...] The maximum proton energy can be explained by the charge-separation electrostatic-field acceleration due to *vacuum heating*.

Snavely et al: "We have concluded that light pressure effects at the front surface [...] could not generate the observed ions because of the clear evidence that the protons are emitted perpendicular to the rear surface(s) of the target."

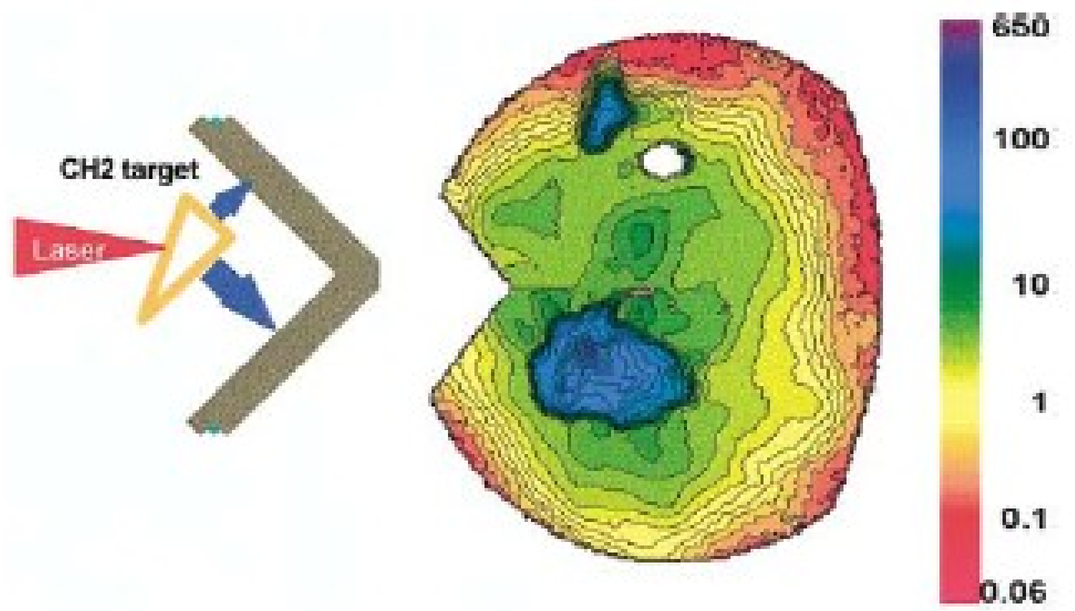

FIG. 4 (color). Contours of dose in krads as a function of angle recorded on a RC film through 300 μm Ta (proton $E >$ 18 MeV). The image clearly shows two proton beams, the larger from the major face and the smaller from the minor face of the wedge.

The Target Normal Sheath Acceleration (TNSA) model of proton acceleration

Physical mechanism:
acceleration in the space-charge electric field generated at the rear surface by "fast" electrons escaping from the target

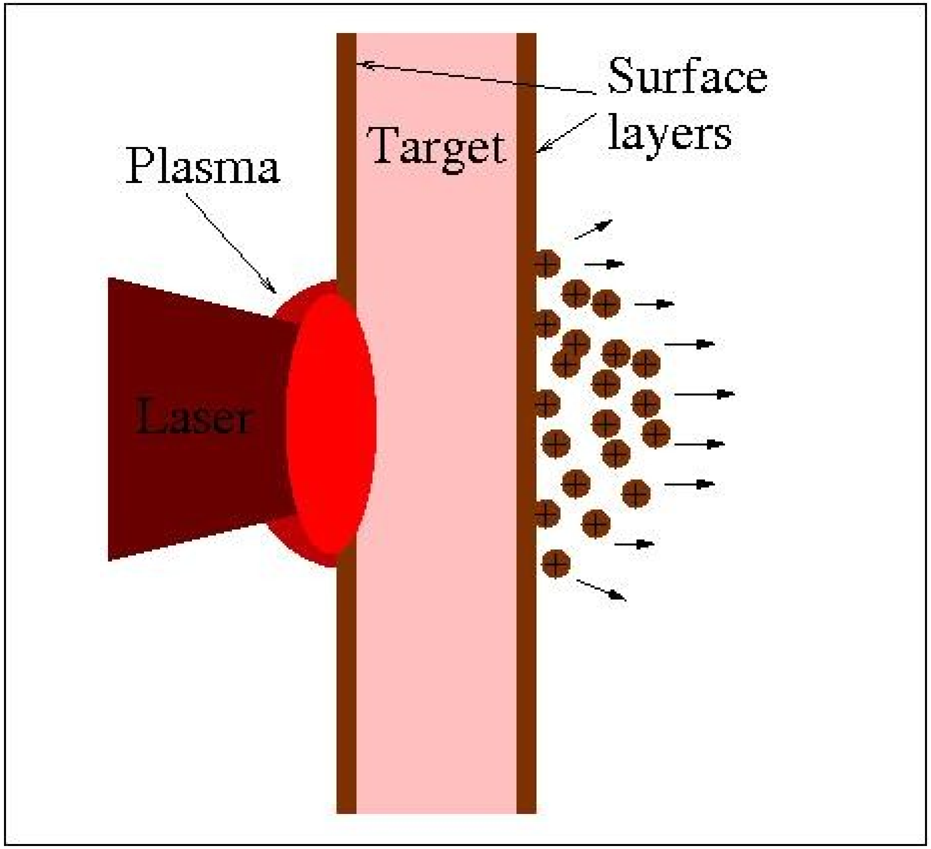

The Target Normal Sheath Acceleration (TNSA) model of proton acceleration

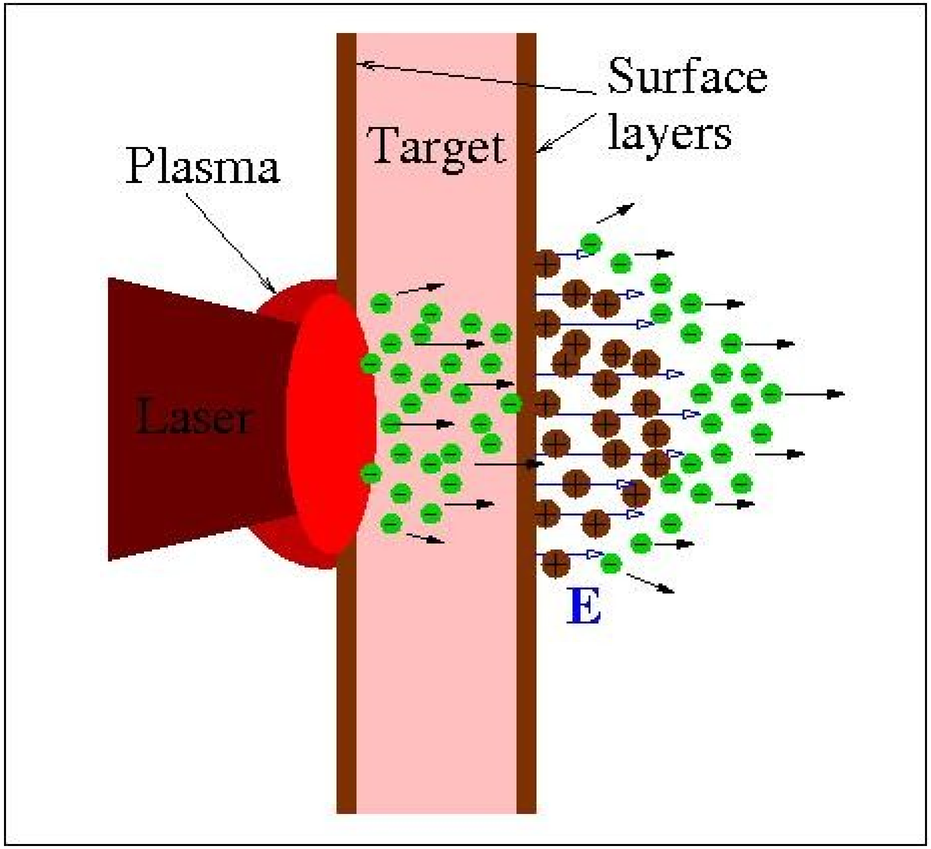

Physical mechanism:
acceleration in the space-charge electric field generated at the rear surface by "fast" electrons escaping from the target

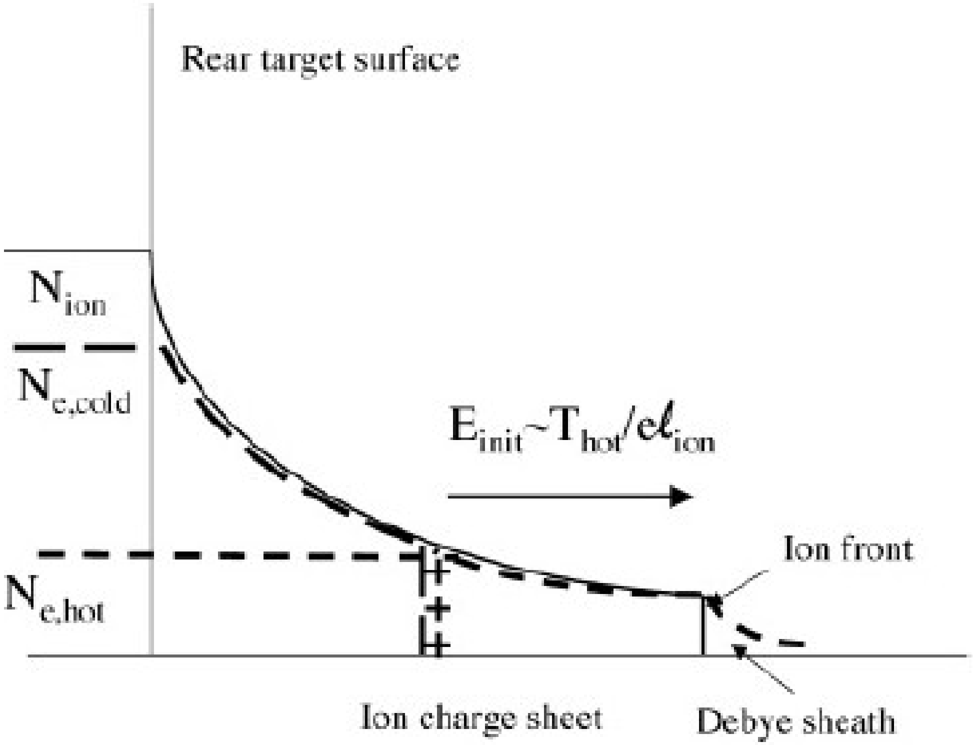

The fast electrons generate an expanding charged layer (Debye sheath)

[S. Wilks et al, Phys. Plasmas **8** (2001) 542]

Modeling of sheath acceleration: the classic problem of plasma expansion in vacuum

Concept: model of the “hot” electrons + “cold” protons as an ideal plasma expanding in vacuum

$$v_{te} = \sqrt{\frac{T_e}{m_e}} > v_{ti} = \sqrt{\frac{T_i}{m_i}} \qquad (m_e \ll m_i)$$

- electrons attempt to leave the (globally neutral) plasma
- space charge unbalance generates an electrostatic field
- the electric field accelerates ions
- asymptotic state: equal velocities $v_i = v_e$

fluid and kinetic models are available in the literature (with simplifying assumptions: 1D geometry, quasi-neutrality, self-similarity, ...)

model geometry (i.e. planar vs. spherical) and input parameters (electron temperature T_e, density n_e ...) are either inferred from or adapted to “experimental” conditions

1D planar, fluid model – I (isothermal)

Analytical approach:
- electrostatic
- fluid ions
- electrons in Boltzmann equilibrium
- step-like, semi-infinite initial density profile

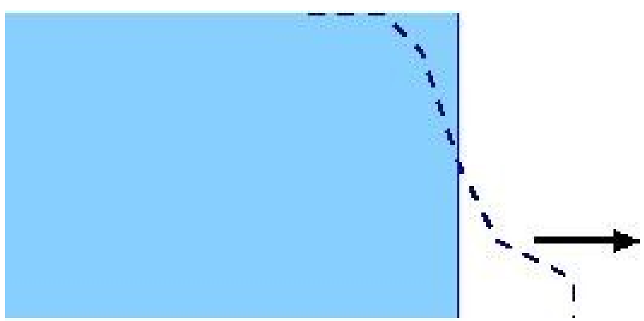

$$n_e = n_0 \exp\left(\frac{e\Phi}{k_B T_e}\right), \qquad \nabla^2\Phi = Zen_i - en_e$$

$$\frac{d\mathbf{v}_i}{dt} = \frac{Ze}{Am_p}\mathbf{E} = -\frac{Ze}{Am_p}\boldsymbol{\nabla}\Phi, \qquad \partial_t n_i = -\boldsymbol{\nabla}\cdot(n_i\mathbf{v}_i)$$

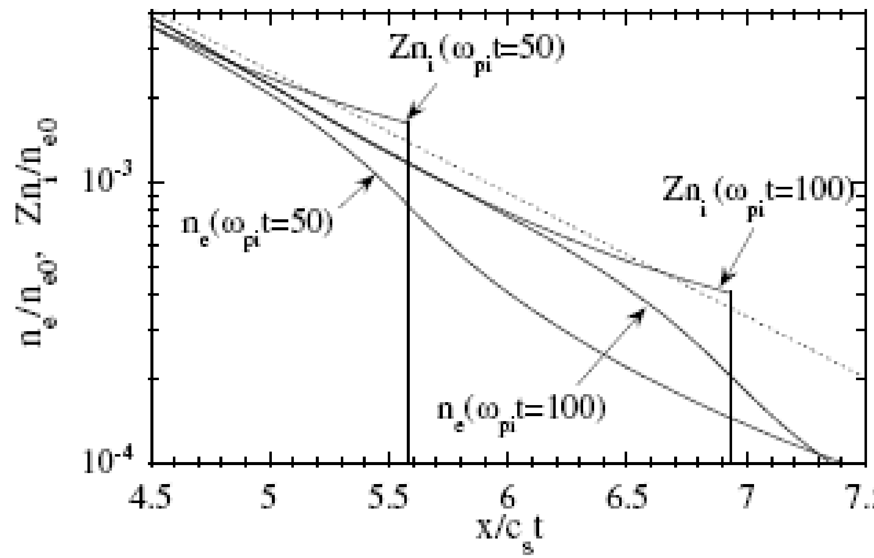

"Mora's formula" from isothermal, semi-infinite slab model
[P.Mora, PRL **90** (2003) 185002]

- diverges with time (infinite energy available!)
- "corrected" assuming finite acceleration time t_p
[J.Fuchs et al, Nature Phys. **2** (2005) 48]

$$v_i \simeq 2c_s \ln\left(\omega_{pi}t_p + \sqrt{\omega_{pi}^2 t_p^2 + 1}\right)$$

$$c_s = \sqrt{\frac{Zk_BT_e}{Am_p}}, \qquad \omega_{pi} = \sqrt{\frac{4\pi Z n_i e^2}{Am_p}}$$

1D planar, fluid model – II (non-isothermal)

Analytical approach:
- electrostatic
- fluid ions
- electrons in Boltzmann equilibrium
- thin plasma slab to account for finite energy

$$n_e = n_0 \exp\left(\frac{e\Phi}{k_B T_e}\right), \qquad \nabla^2\Phi = Zen_i - en_e$$

$$\frac{d\mathbf{v}_i}{dt} = \frac{Ze}{Am_p}\mathbf{E} = -\frac{Ze}{Am_p}\boldsymbol{\nabla}\Phi, \qquad \partial_t n_i = -\boldsymbol{\nabla}\cdot(n_i\mathbf{v}_i)$$

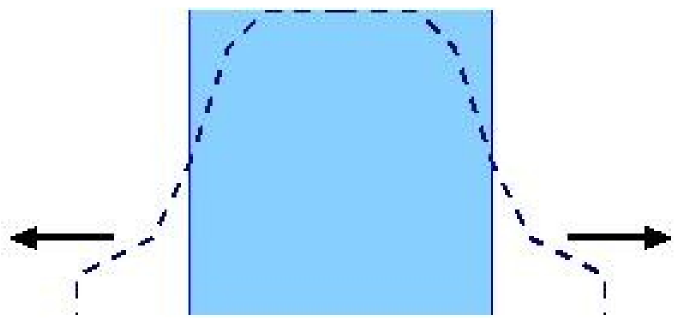

- T_e decreases in time (adiabatic cooling)

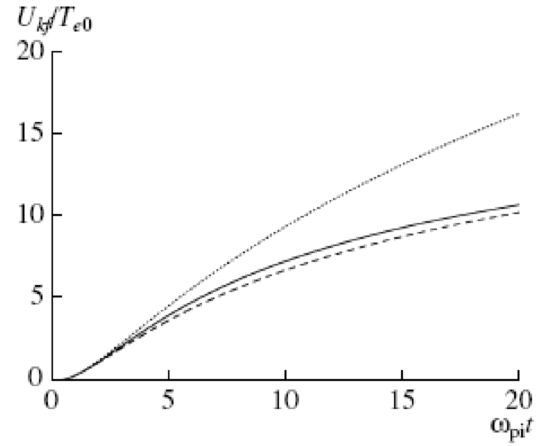

Fig. 3. The kinetic energy acquired by the fastest ion during the expansion of a slab of total thickness $2a = 40$ as predicted by the numerical simulations (solid line), by the analytical model (dashed line), and by the semi-infinite model [11] (dotted line).

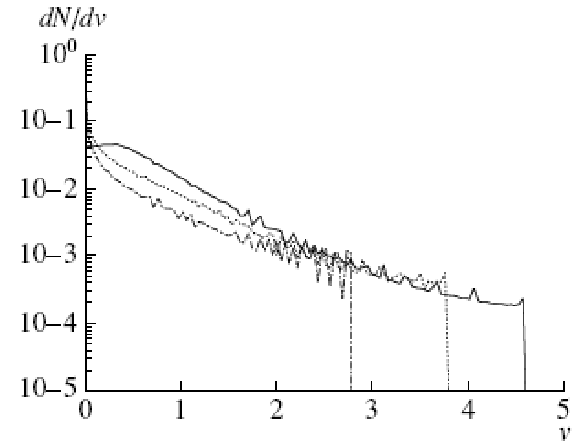

Fig. 4. Ion velocity spectrum at $\tau = 5$ (dashed line), $\tau = 10$ (dotted line), and $\tau = 20$ (solid line). The initial slab total size is $2a = 40$ and v is normalized to the initial sound speed.

Excellent agreement with numerical PIC results

S.Betti, F.Ceccherini, F.Cornolti, F.Pegoraro, Plasma Phys. Control. Fusion **47** (2005) 521;
F.Ceccherini, S.Betti, F.Cornolti, F.Pegoraro, Laser Physics **16** (2006) 1

How to diagnose the electric fields directly?
Idea: use the protons as a probe

Due to high laminarity the proton beam has **imaging properties**

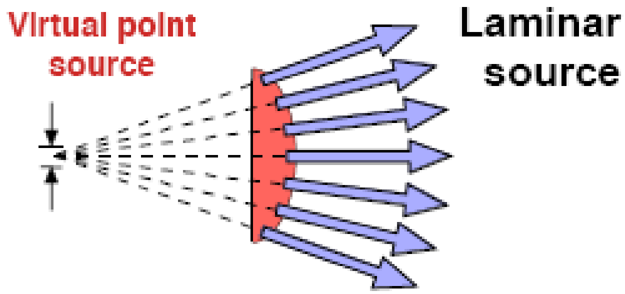

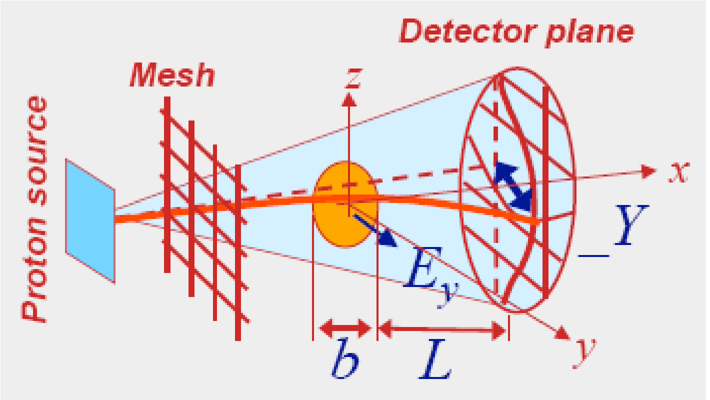

The short duration of the proton burst allows **picosecond temporal resolution**

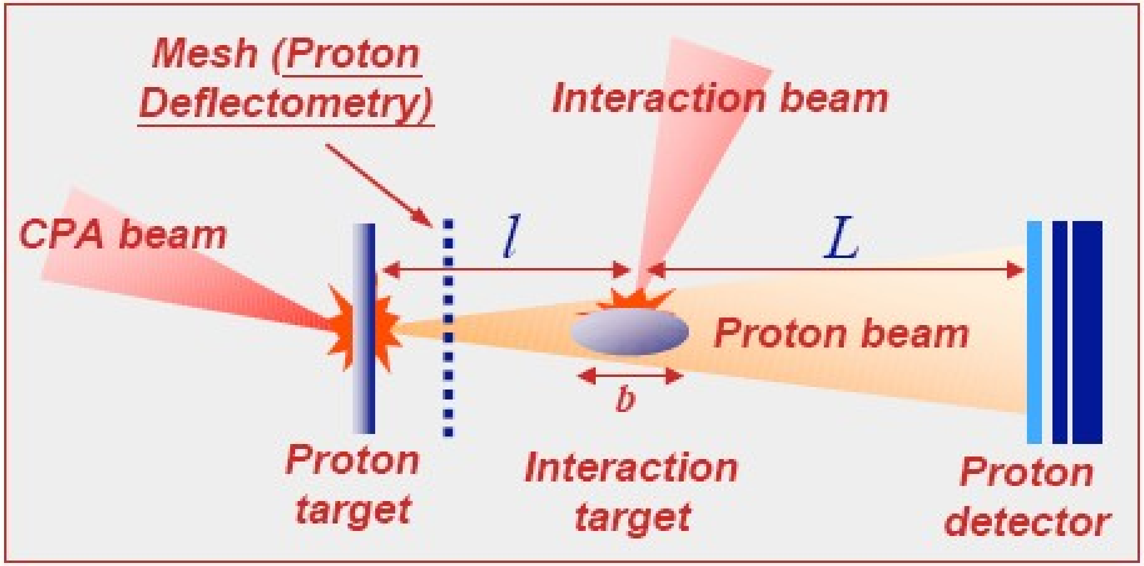

Protons of a given energy will cross the probed object at a particular time.
An energy-resolving detector (e.g. Radiochromic Film) thus provides **multiframe capability**

Borghesi et al, Phys.Plasmas **9** (2002) 2214
Borghesi et al, Phys.Rev.Lett. **92** (2004) 055003
Cowan et al, Phys.Rev.Lett. **92** (2004) 204851

In a laser-plasma experiment the proton probe is easily **synchronized with the interaction** (*more in tomorrow's talk*)

Experimental detection of sheath fields using the proton diagnostic

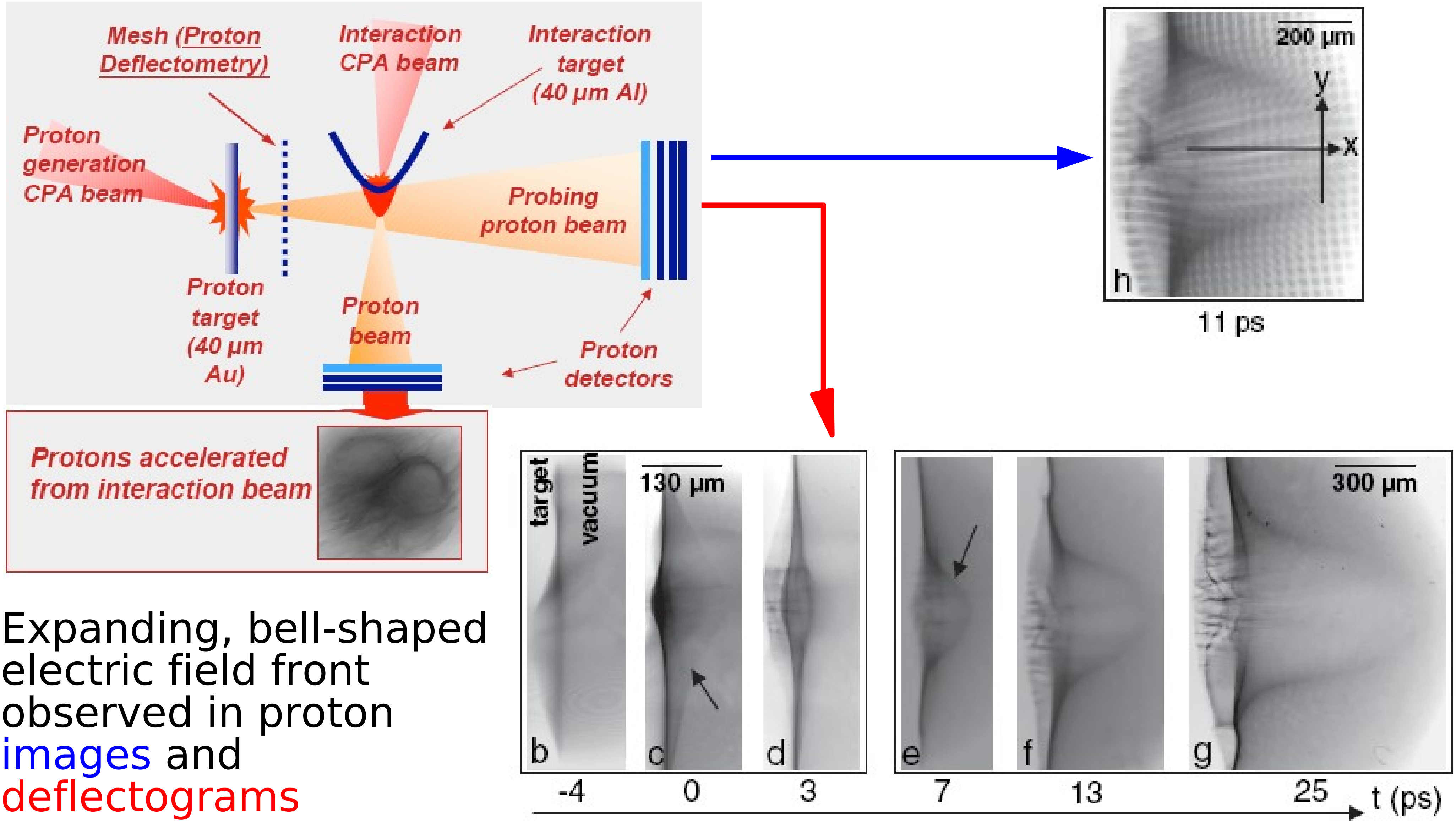

Expanding, bell-shaped electric field front observed in proton images and deflectograms

L. Romagnani, J. Fuchs, M. Borghesi, P. Antici, P. Audebert, F. Ceccherini, T. Cowan, T. Grismayer, S. Kar, A. Macchi, P. Mora, G. Pretzler, A. Schiavi, T. Toncian, O. Willi, Phys. Rev. Lett. **95** (2005) 195001

Experimental detection of sheath fields using the proton diagnostic

Experimental results have been compared with PIC simulations using the plasma expansion model.

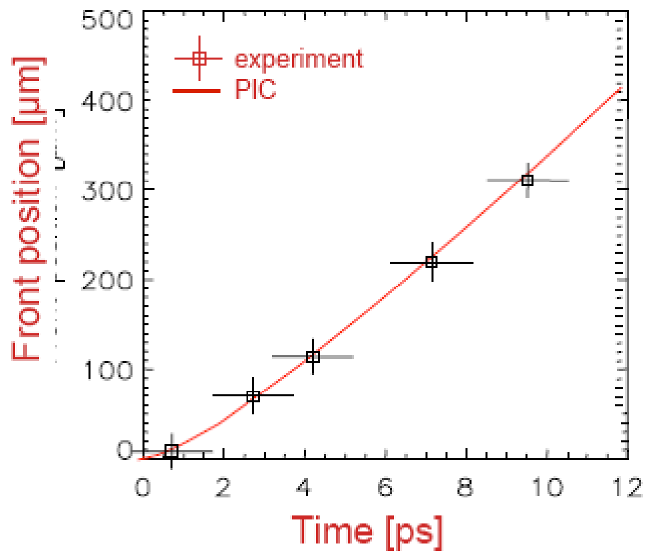

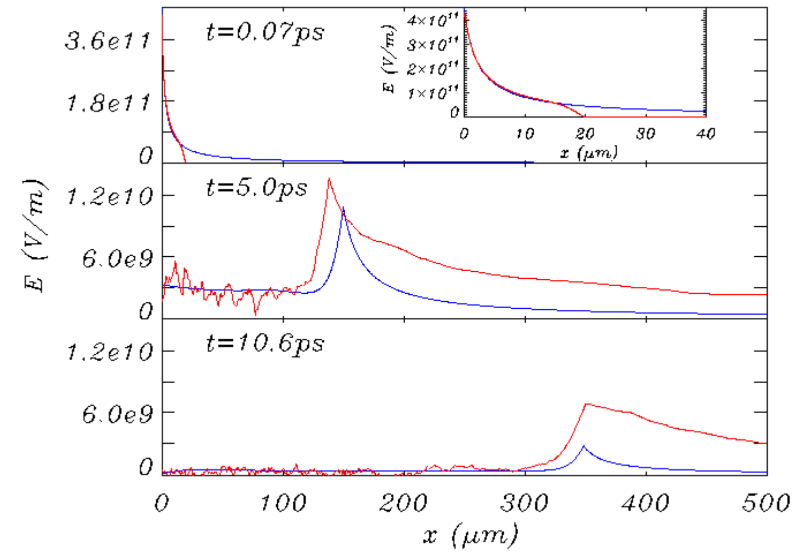

Particle tracing simulations of proton deflection in the PIC fields (plus an “heuristic” modeling of the 2D expansion) fit well experimental images and deflectrograms

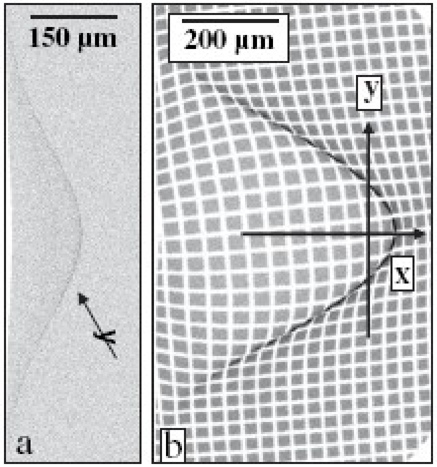

Comparison of fluid and kinetic (PIC) results show the importance of kinetic and non-thermal effects in the plasma expansion

L. Romagnani, J. Fuchs, M. Borghesi, P. Antici, P. Audebert, F. Ceccherini, T. Cowan, T. Grismayer, S. Kar, A. Macchi, P. Mora, G. Pretzler, A. Schiavi, T. Toncian, O. Willi, Phys. Rev. Lett. **95** (2005) 195001

Observed energy scaling in TNSA experiments

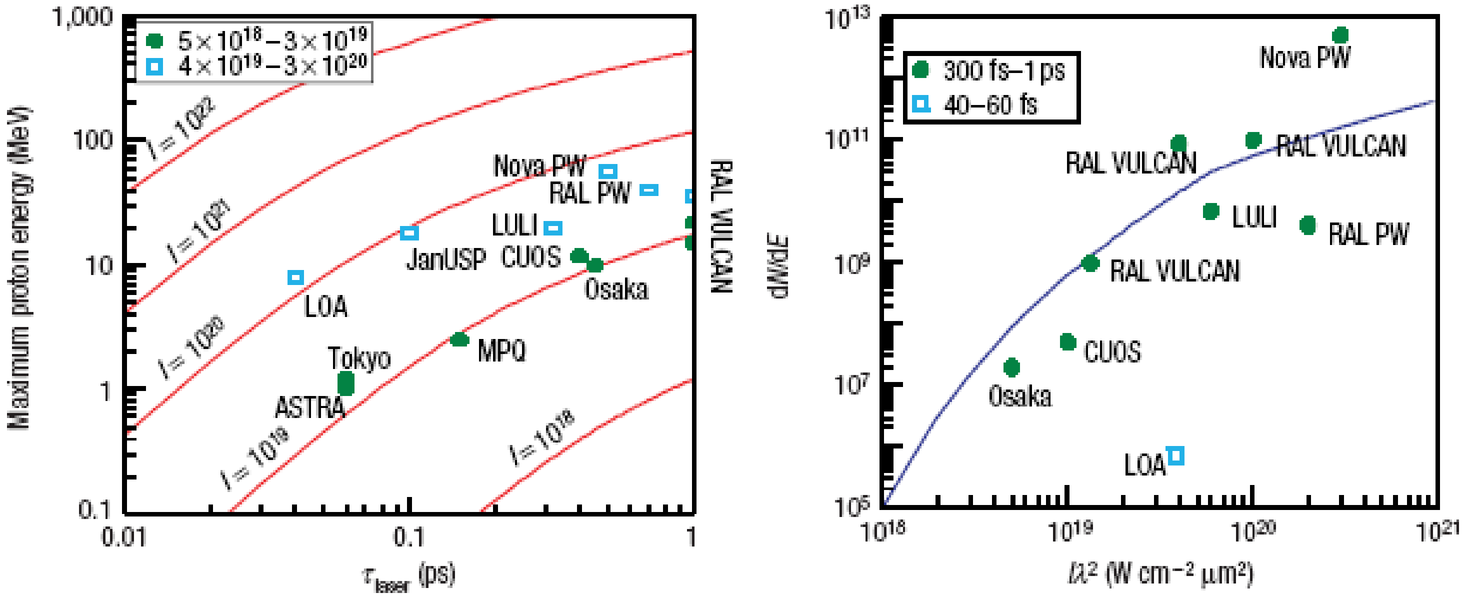

Scaling of ion energy and number vs. pulse duration and irradiance $\sim I^{1/2}$

M.Borghesi et al, Fusion Sci.Tech. **49** (2006) 412; J. Fuchs et al, Nature Physics **2** (2005) 48 .

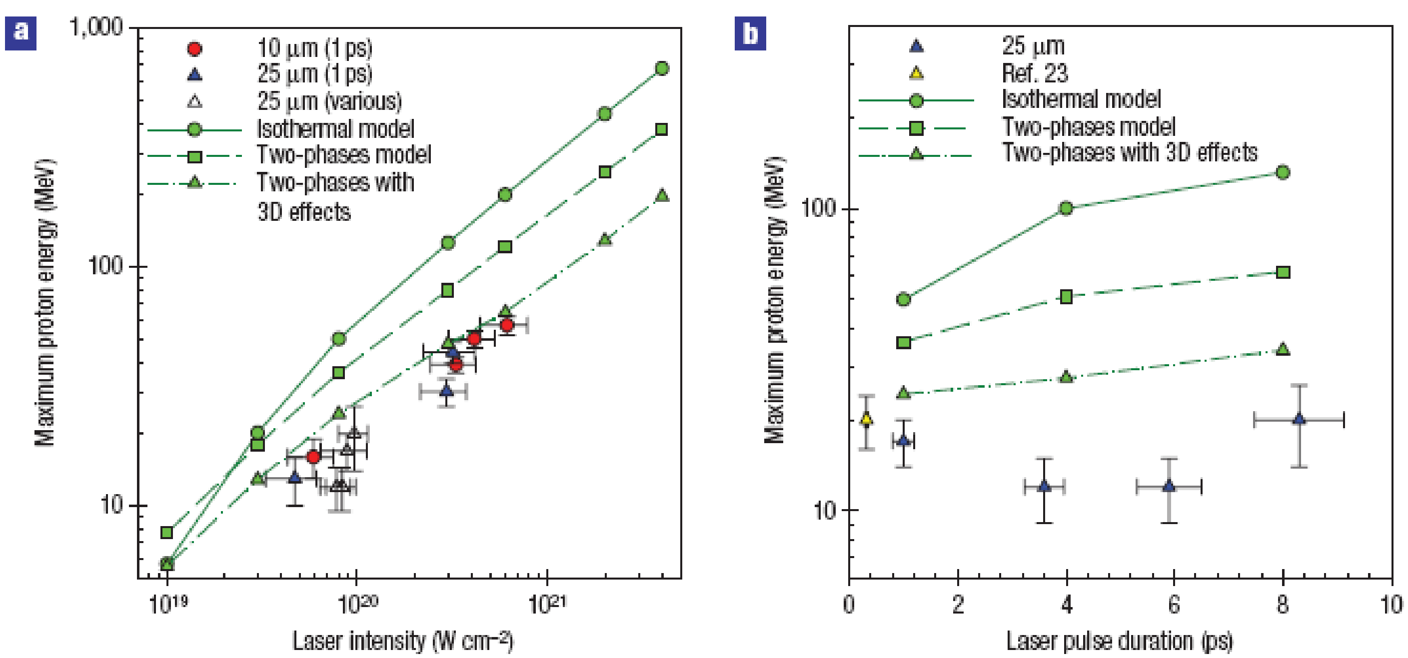

Weaker scaling found at higher intensities (up to 6×10^{20} W/cm^2)

L.Robson et al, Nature Physics **3** (2007) 58

Target microstructuring for spectral optimization and ion species selection

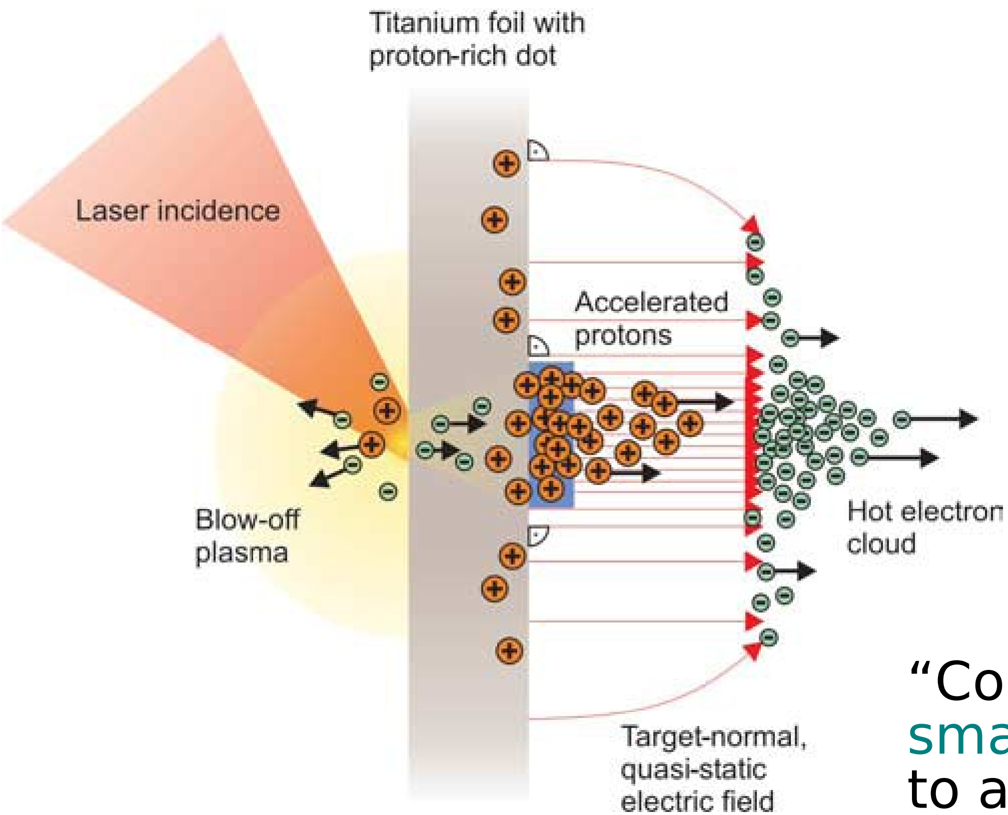

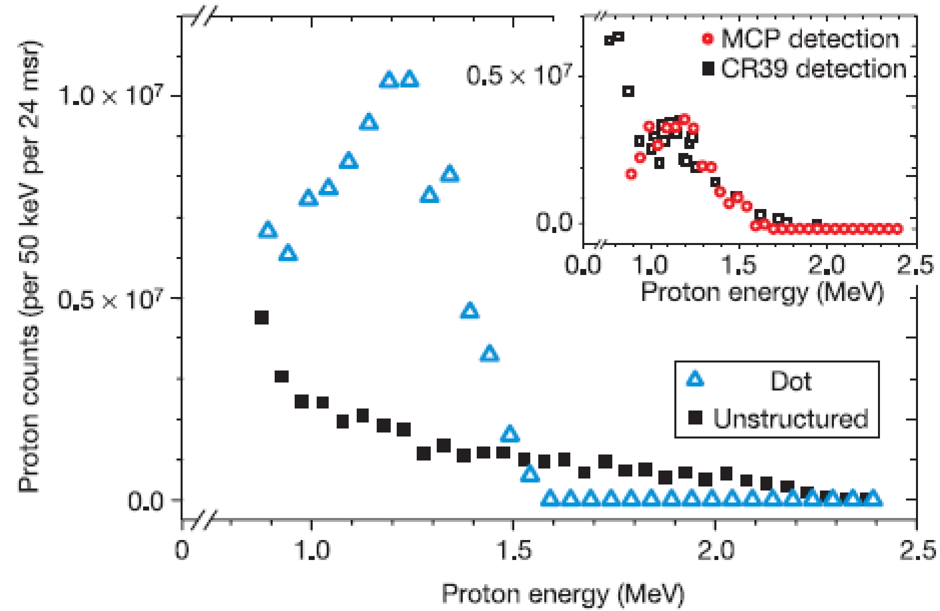

“Confining” the hydrogen content in a small microdot on the rear surface leads to a narrower energy spectrum of protons
H. Schwoerer et al, Nature **439** (2006) 445

A similar microstructuring plus “decontamination” of hydorgen allows the acceleration of Carbon ions
B. Hegelich et al, Nature **439** (2006) 441

Open problems: shot reproducibility, repetition rate, increase energy, reduce spectral width, ...

TNSA-bases devices for dynamic control of protons

Concept: achieve **focusing** and **energy selection** of the proton beam by “external” devices or by “target engineering”

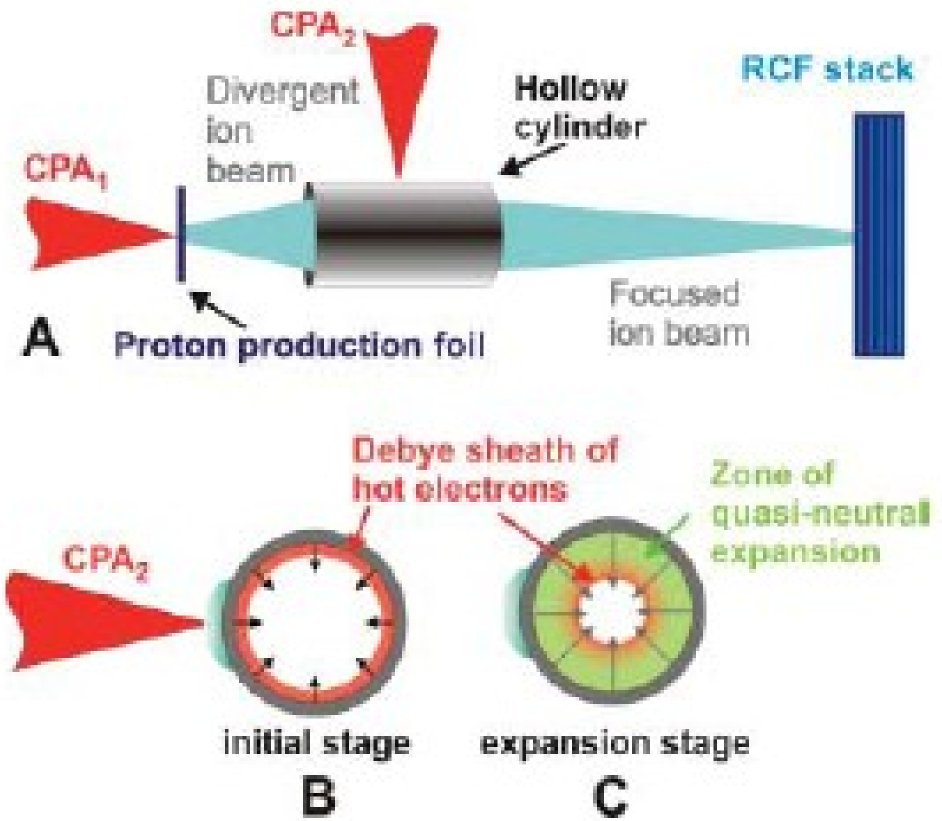

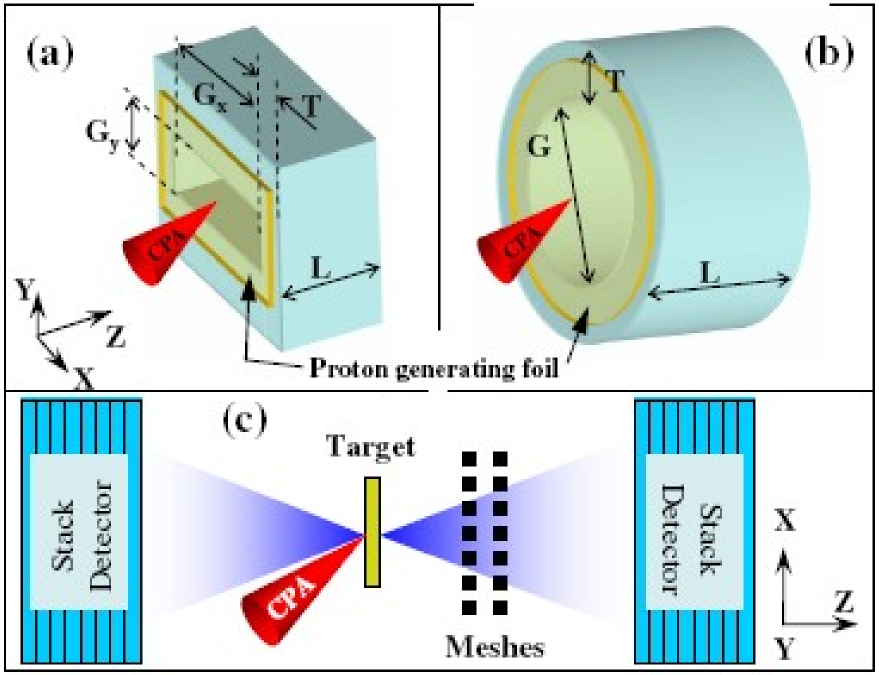

Laser-driven cylindrical microlens
Toncian et al., Science **312** (2006) 410

Shaped targets designed as **electrostatic (*) lenses**
Kar et al., PRL **100** (2008) 105004

(*) Possible role of **electromagnetic** effects:
K.E.Quinn et al, PRL **102**, 194801 (2009)

Observation of "backward" TNSA protons

Most experiment are affected by the laser *prepulse*: the interaction occurs with a preformed, inhomogeneous plasma rather than with the solid-density, step-like target

For "high-contrast", prepulse-free measurements, the density profile is sharp also at the front side: a "symmetrical" TNSA in both forward and backward directions is observed for thin targets (electrons have time to reflux back)

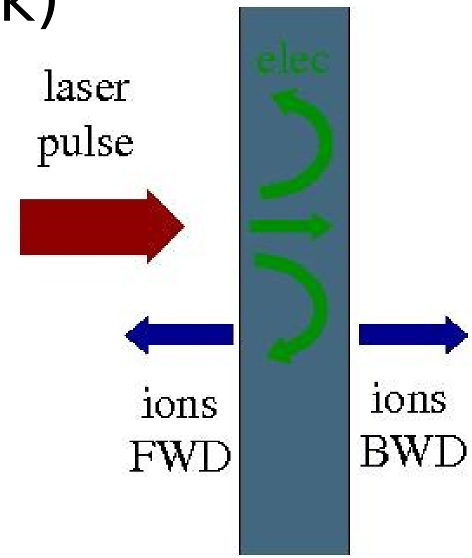

T.Ceccotti et al, PRL **99** (2007) 185002

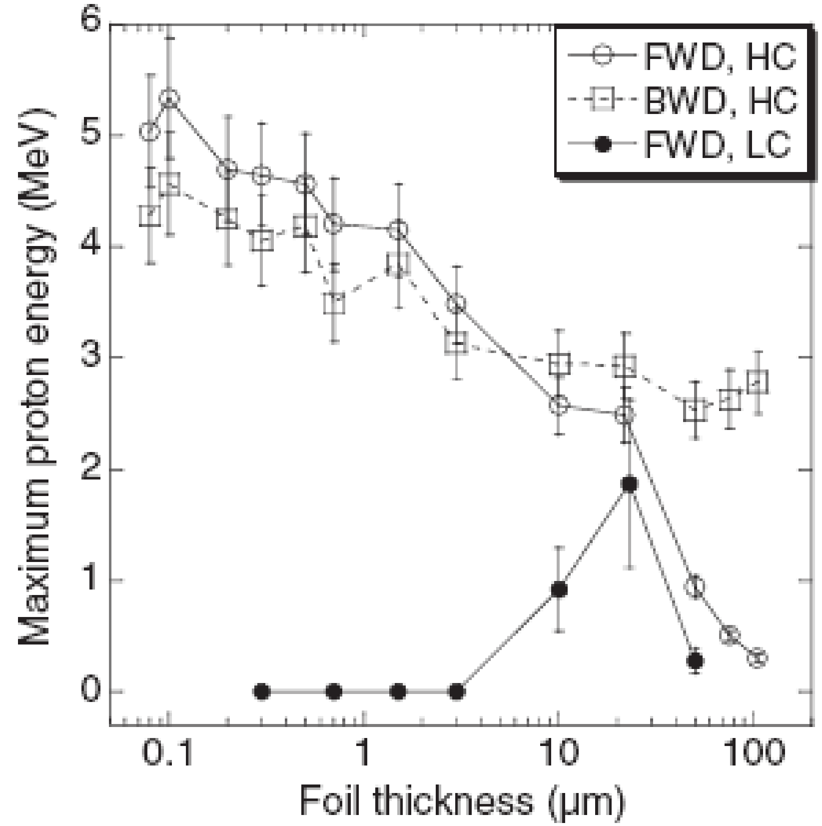

FIG. 1. Variation of maximum detectable proton energy as a function of target thickness. The FWD and BWD emissions for a laser contrast of 10^{10} (10^{6}) and intensity of 5×10^{18} W/cm^2 (10^{19} W/cm^2) are represented, respectively, by open (solid) circles and squares. Lines are a guide for the eye.

Very thin targets + ultrahigh intensities: Radiation Pressure effects?

In petawatt ($I \sim 10^{20}$ W/cm^2) experiments for "quite thin" targets a highly collimated dense plasma jet from the rear side is observed

Interpretation:
due to front side ions pushed forward by the radiation pressure of the laser pulse

(absence of jet for larger thickness ascribed to collisional ion stopping in the target)

S.Kar, M.Borghesi, S.V.Bulanov, A.Macchi, M.H.Key,T.V.Liseykina, A.J.MacKinnon, P.K.Patel, L.Romagnani, A.Schiavi , O.Willi, PRL **100** (2008) 225004

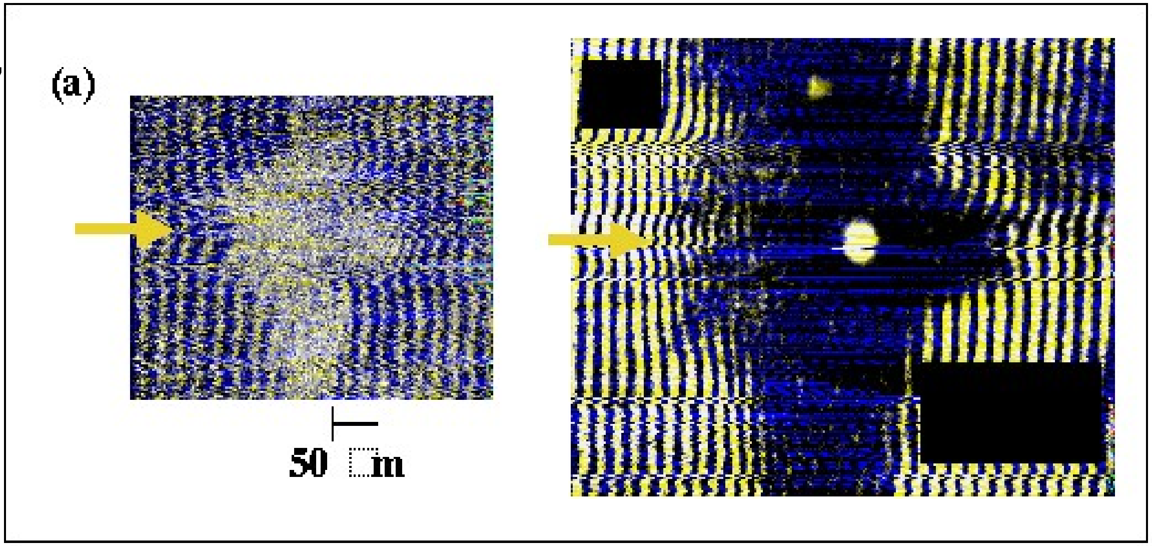

Interferometry data

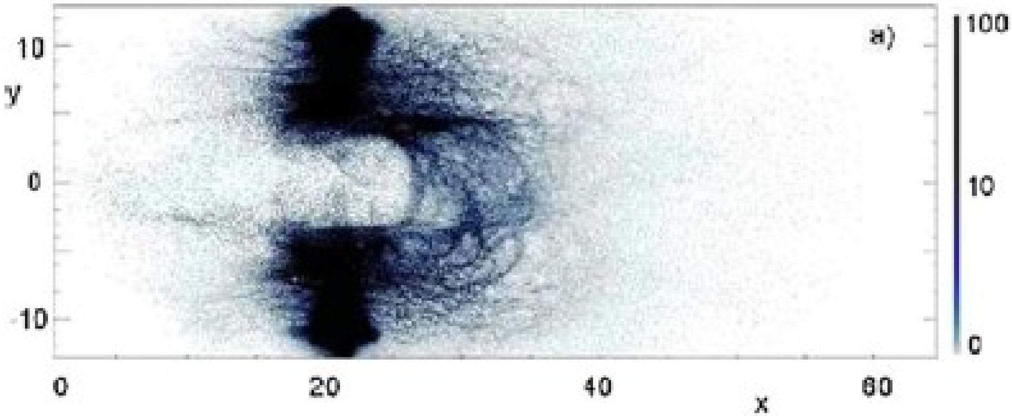

2D PIC simulation (S.V. Bulanov)

Simulations suggest regime transition at intensities ~ 10^{21} W/cm^2

Results from "multi-parametric" PIC simulations:

- for maximal ion energy an optimal areal density $n_e d$ exists for given intensity I
- ion energy scales with laser energy ε_L
  as $\varepsilon_L^{1/2}$ for $I < 10^{21}$ W/cm^2
  as ε_L for $I > 10^{21}$ W/cm^2
- transition is explained by the dominance of Radiation Pressure Acceleration

T.Esirkepov et al, PRL **96** (2006) 105001

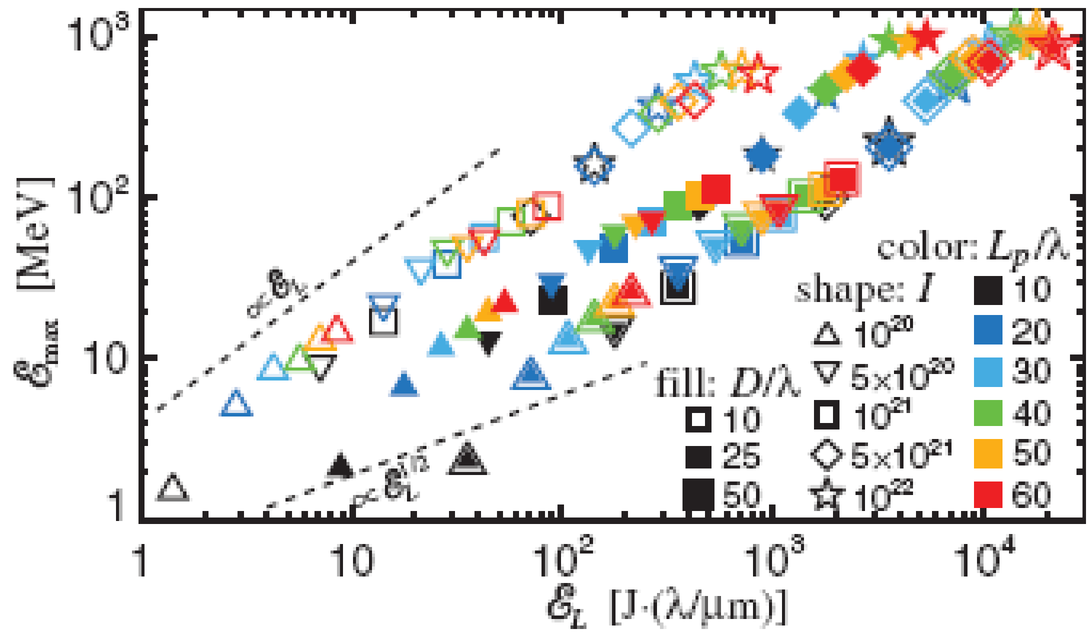

FIG. 3 (color). Proton maximum energy vs laser pulse energy for $l = \lambda$, $n_e = 100 n_{cr}$. The dashed lines exemplify possible scalings.

Relativistic ions: the “*Laser-Piston*” regime

Ultra-relativistic interaction regime
“dominated by radiation pressure”:
efficient generation of relativistic, highly monoenergetic and collimated ions from ultrathin foils

T.Esirkepov, M.Borghesi, S.V.Bulanov, G.Mourou, T.Tajima, PRL **92**, 175003 (2004)

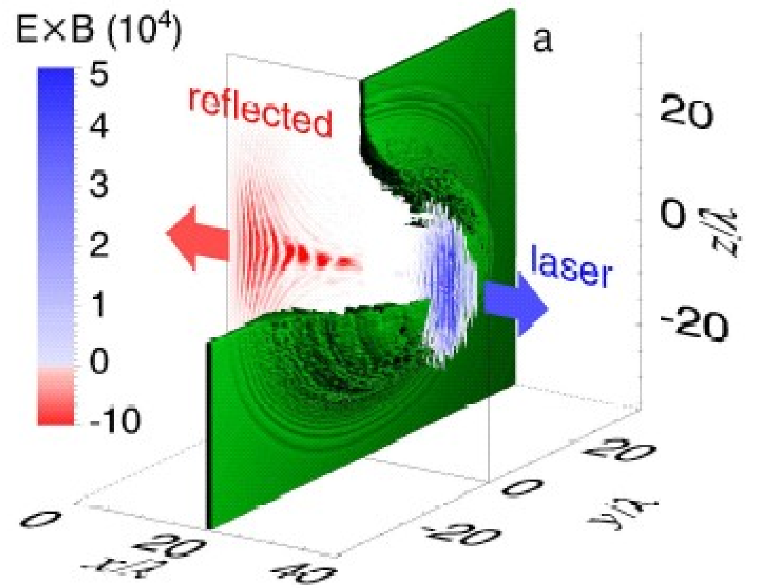

Required laser intensity

$$I \geq 10^{23}\ \mathrm{W/cm^2}$$

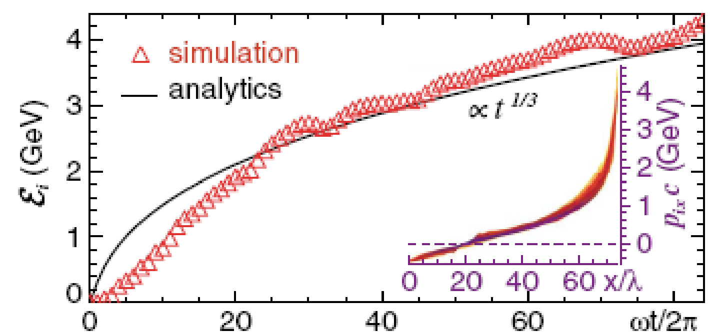

The foreseen ion beam parameters make this attractive as a driver of low-energy neutrino sources for studies of CP violation in $\nu_\mu \Rightarrow \nu_e$ oscillations

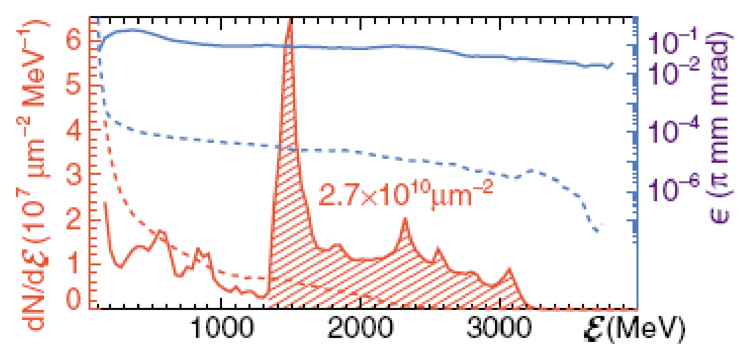

S.V.Bulanov, T.Esirkepov, P.Migliozzi, F.Pegoraro, T.Tajima, F.Terranova, NIM A **540**, 133 (2005)

Radiation Pressure Acceleration: transfering the momentum of light to matter

The acceleration of a massive mirror by light pressure is particularly efficient when the velocity becomes close to the speed of light (this suggested the “visionary” application of a laser-propelled rocket 44 years ago:)

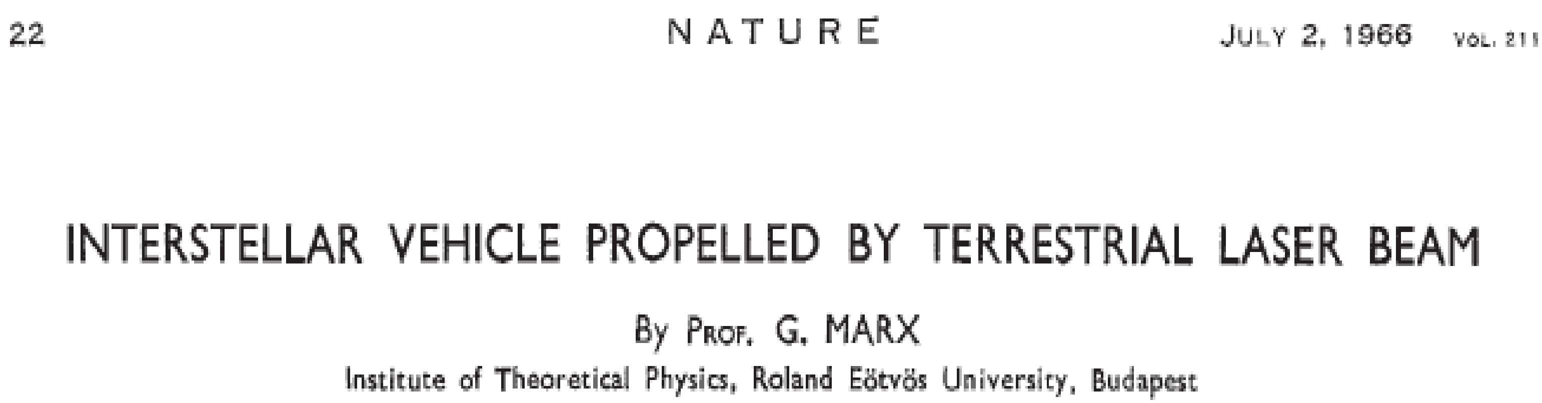
22 NATURE JULY 2, 1966 VOL. 211

INTERSTELLAR VEHICLE PROPELLED BY TERRESTRIAL LASER BEAM

By PROF. G. MARX

Institute of Theoretical Physics, Roland Eötvös University, Budapest

A breakthrough in efficiency is expected as we enter in the relativistic regime

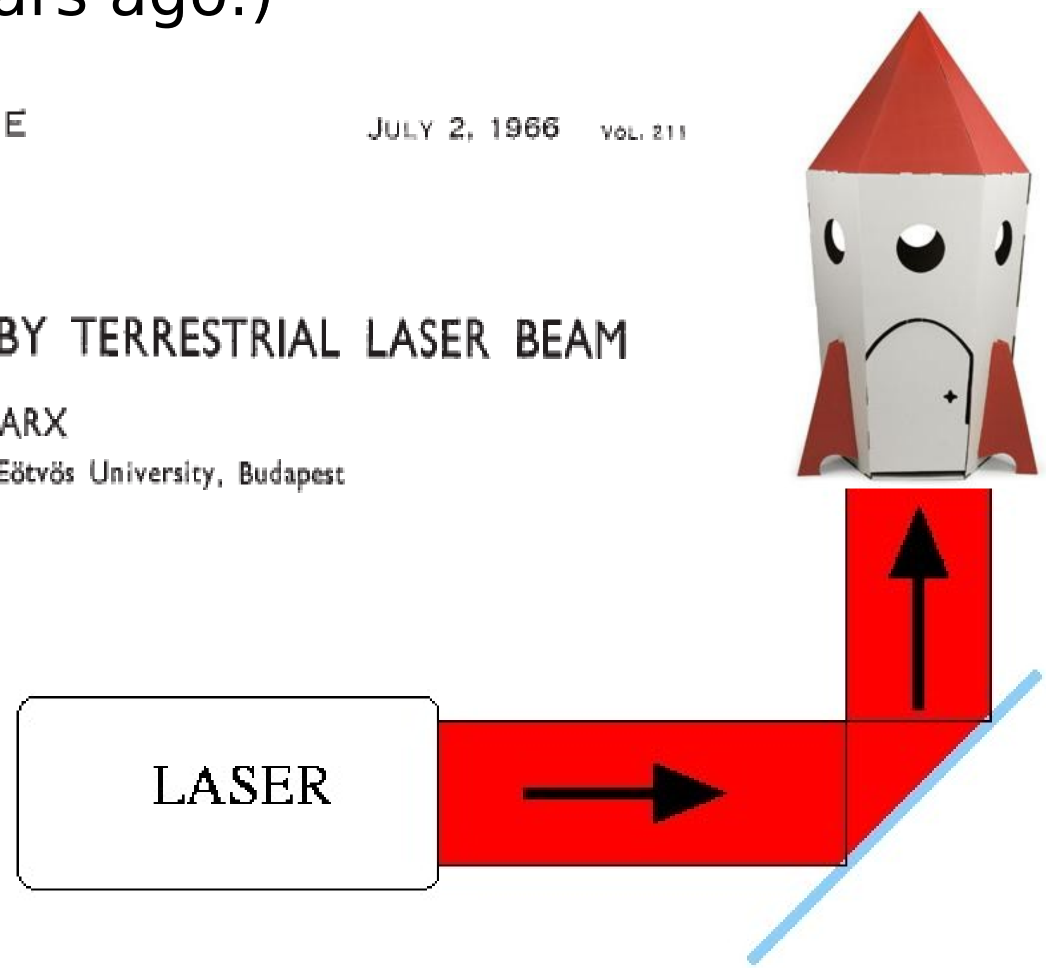

The "Light Sail" or (Accelerating Mirror) model

Model: a perfectly reflecting, rigid mirror of mass $M = \rho \ell S$ boosted by a plane light wave

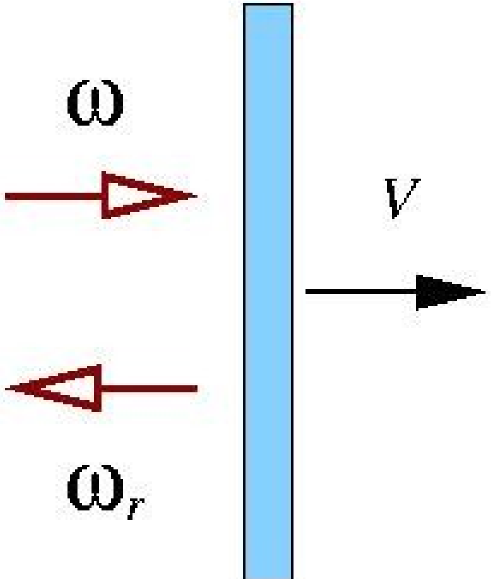

Mirror velocity as a function of the laser pulse intensity I and duration τ and of the surface density $n_e \ell$ of of the target:

$$\beta(t) = \frac{(1+\mathcal{E})^2 - 1}{(1+\mathcal{E})^2 + 1}, \qquad \mathcal{E} = \frac{2F(t)}{\rho \ell c^2} = 2\pi \frac{Z}{A} \frac{m_e}{m_p} \frac{a_0^2 \tau}{\zeta}$$

$$F(t) = \int_0^t I(t')dt' \propto a_o^2 \tau, \qquad \zeta = \pi \frac{n_e}{n_c} \frac{\ell}{\lambda}$$

Energy per nucleon scales with $I\tau$

G.Marx, Nature **211**, 22 (1966)
J.F.L.Simmons and C.R.McInnes, Am.J.Phys. **61**, 205 (1993)

The "Light Sail" or (Accelerating Mirror) model

The efficiency of the acceleration process can be obtained by a simple argument of conservation of "number of photons" plus the Doppler shift of the reflected light:

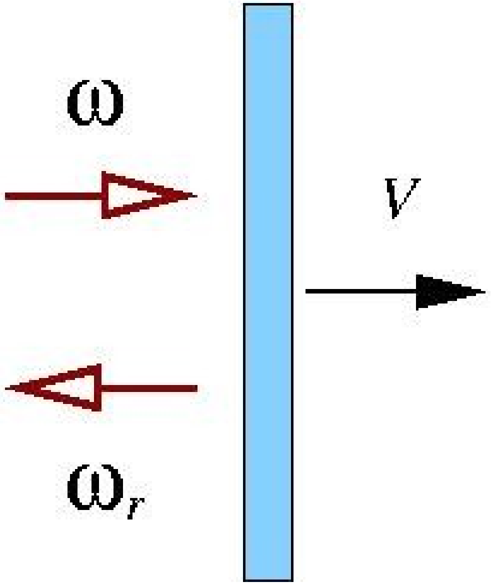

$$N = \frac{IS\tau}{\hbar\omega}, \qquad \omega_r = \omega\frac{1-\beta}{1+\beta}$$

$$\eta = \frac{\mathcal{E}_{\rm abs}}{\mathcal{E}_{\rm laser}} = \frac{N\hbar(\omega-\omega_r)}{IS\tau} = \frac{2\beta}{1+\beta}$$

$$\beta \to 1 \Rightarrow \eta \to 1$$

100% efficiency in the relativistic limit

G.Marx, Nature **211**, 22 (1966)
J.F.L.Simmons and C.R.McInnes, Am.J.Phys. **61**, 205 (1993)

Maximize the effect of Radiation Pressure: the “optical mill” (Solar radiometer) example

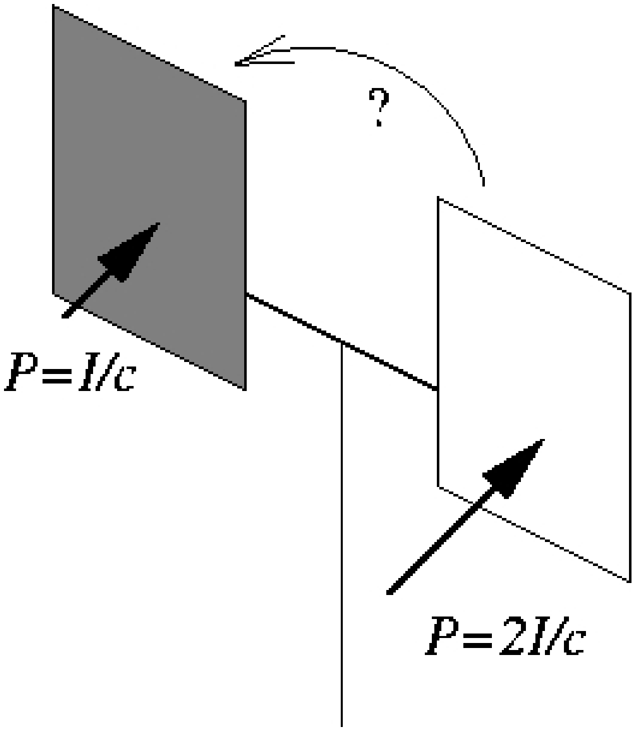

The mill spins in the opposite direction to what we'd expect thinking of P_{rad} only: the heating of the **black** (absorbing) surface increases the thermal pressure of the background gas (imperfect vacuum in the bulb!)

In the high-intensity irradiation of a solid-density (plasma) target, “heating” is due to “irreversible” energy absorption into electrons (those electrons driving in turn TNSA)

Is there a way to suppress (reduce) electron heating?

How to "switch off" fast electrons

Forced oscillations of the electrons across the plasma-vacuum interface ($L << \lambda$) driven by the 2ω component of the **J**x**B** force (normal incidence) are non-adiabatic and lead to electron acceleration ("vacuum heating" effect at normal incidence)

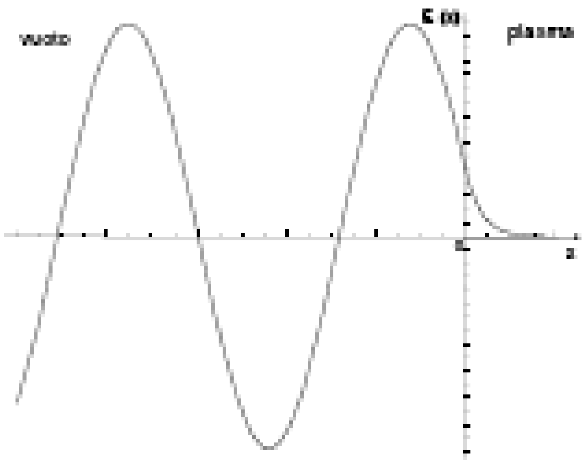

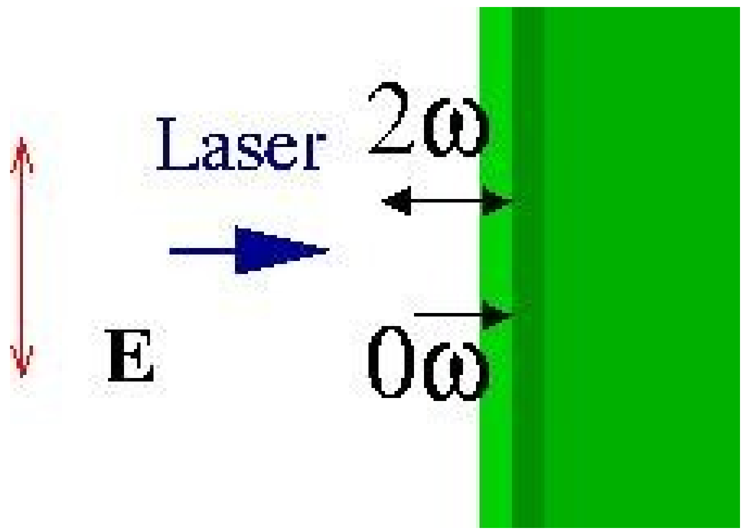

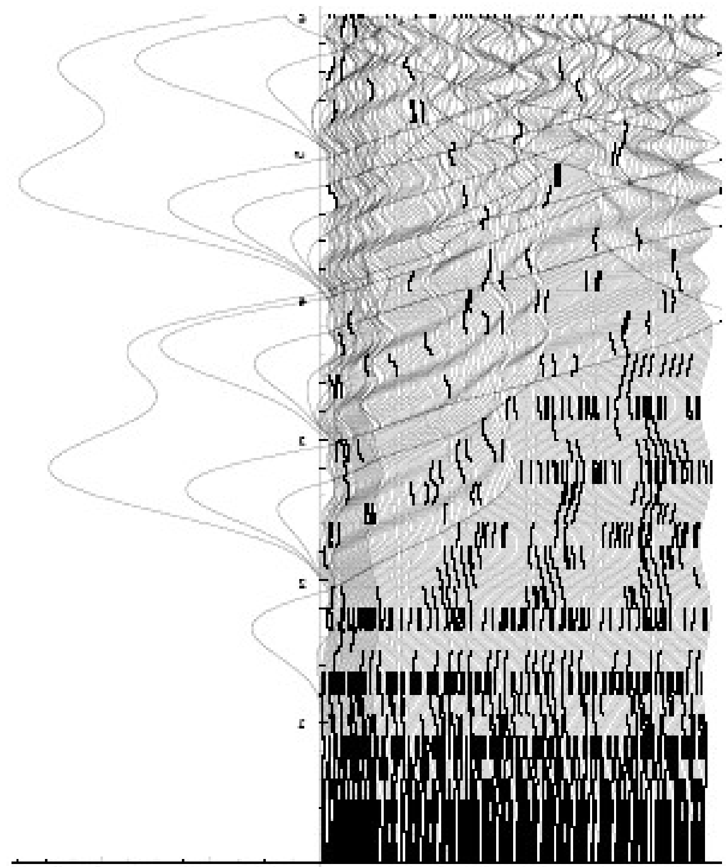

S. Tuveri, tesi di Laurea, 2006

F.Brunel, PRL **59** (1987) 52
P. Gibbon, *Short Pulse Laser Interaction with Matter* (Imperial College Press, 2005)
P. Mulser, D. Bauer, and H. Ruhl, PRL **101** (2008) 225002

How to “switch off” fast electrons

For circular polarization,
the 2ω component of the **J**x**B**
force vanishes:
- inhibition of electron acceleration
- **“direct” ion acceleration**

i.e. “dominance” of Radiation Pressure at any laser intensity!

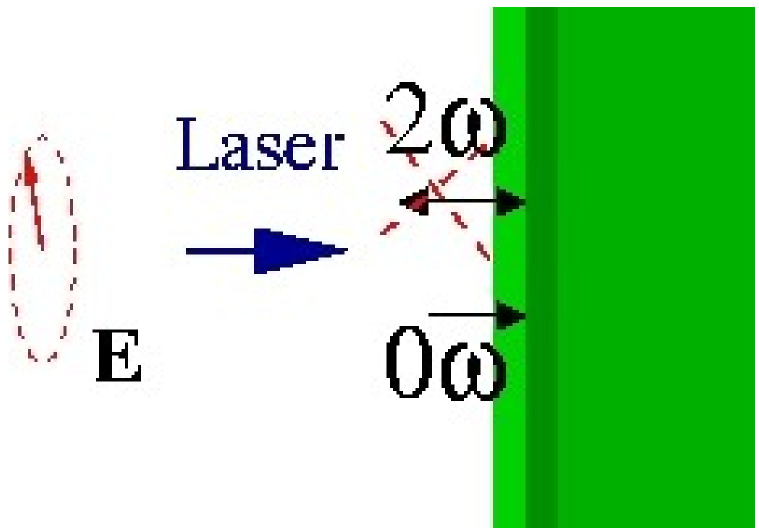

A.Macchi, F.Cattani, T.V.Liseikina, F. Cornolti, PRL **94**, 165003 (2005)

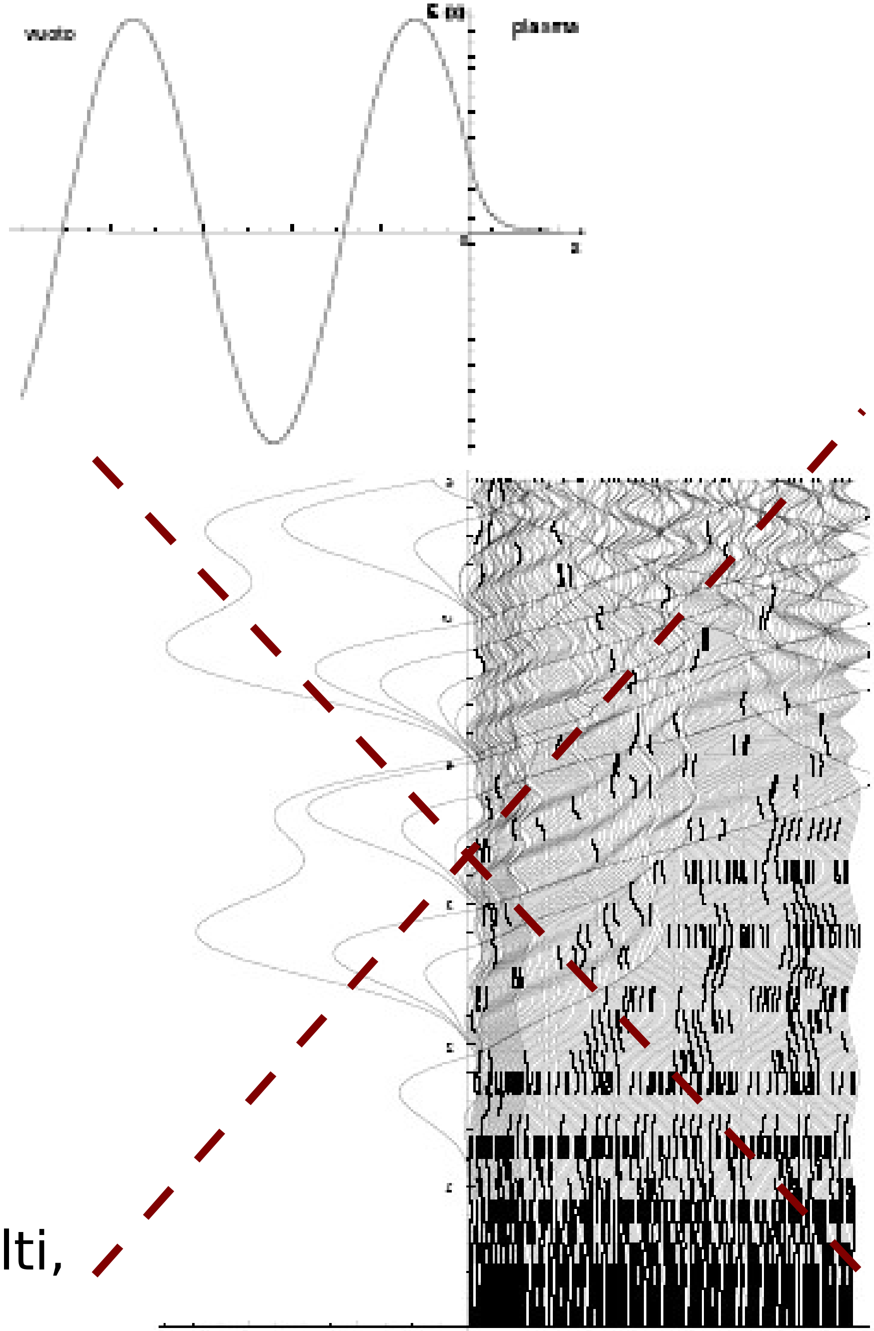

S. Tuveri, tesi di Laurea, 2006

Simulation of thin foil acceleration: CP vs. LP

- Carbon target, thickness d=0.04μ m, n_e=250n_c=4.3×10^{23} cm^{-3}
- Laser: 26 fs pulse, I=1.8×10^{20} W/cm^2

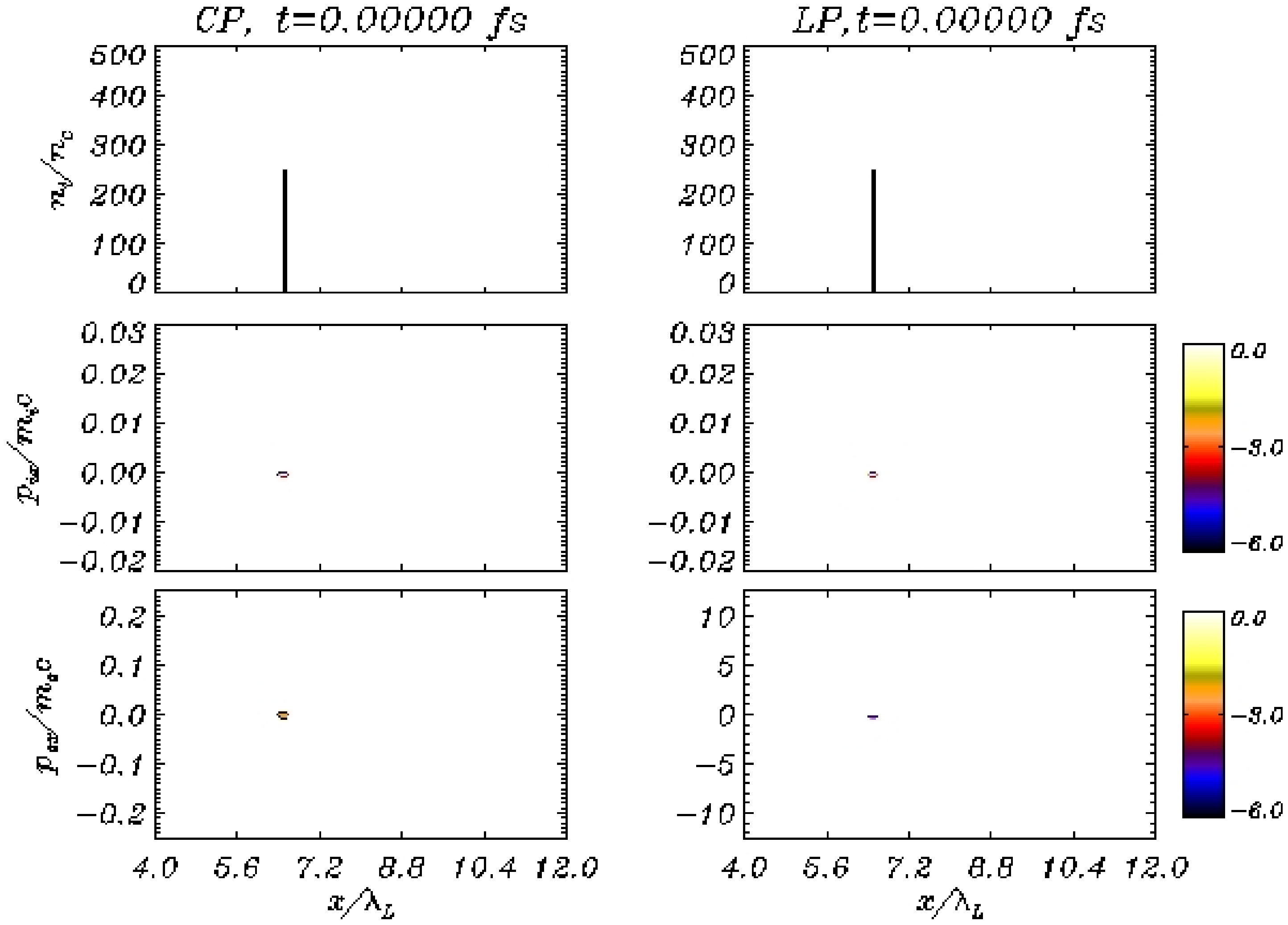

CP: Electrons are "cold" (~keV)
Foil accelerated as a whole

LP: Electrons are "hot" (~MeV)
foil explodes, broad ion spectrum

Simulation of thin foil acceleration: CP vs. LP

- Carbon target, thickness d=0.04μ m, n_e=250n_c=4.3×10^{23} cm^{-3}
- Laser: 26 fs pulse, I=1.8×10^{20} W/cm^2

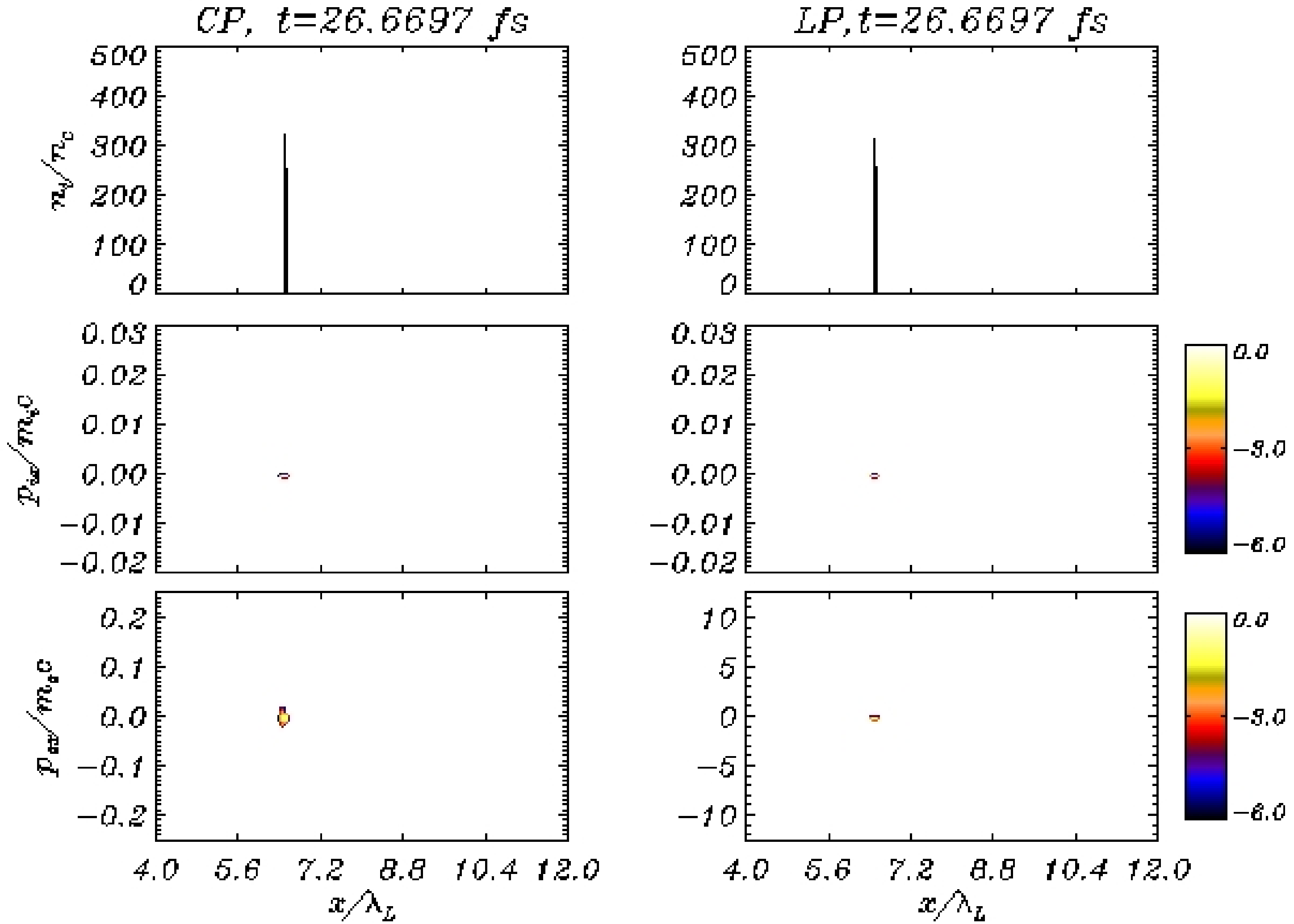

CP: Electrons are “cold” (~keV)
Foil accelerated as a whole

LP: Electrons are “hot” (~MeV)
foil explodes, broad ion spectrum

Simulation of thin foil acceleration: CP vs. LP

- Carbon target, thickness d=0.04μ m, n_e=250n_c=4.3×10^{23} cm^{-3}
- Laser: 26 fs pulse, I=1.8×10^{20} W/cm^2

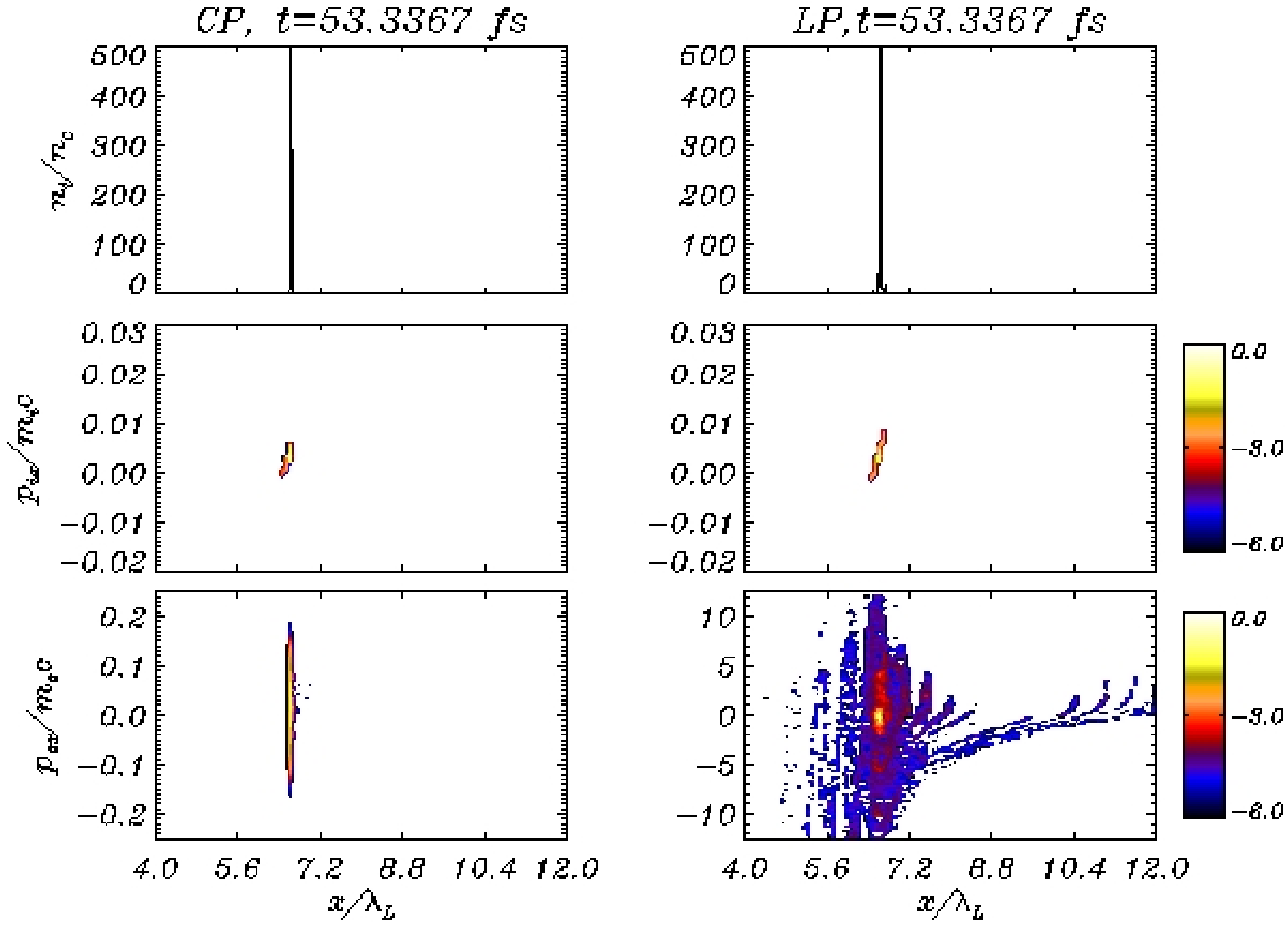

CP: Electrons are "cold" (~keV)
Foil accelerated as a whole

LP: Electrons are "hot" (~MeV)
foil explodes, broad ion spectrum

Simulation of thin foil acceleration: CP vs. LP

- Carbon target, thickness d=0.04μ m, n_e=250n_c=4.3×10^{23} cm^{-3}
- Laser: 26 fs pulse, I=1.8×10^{20} W/cm^2

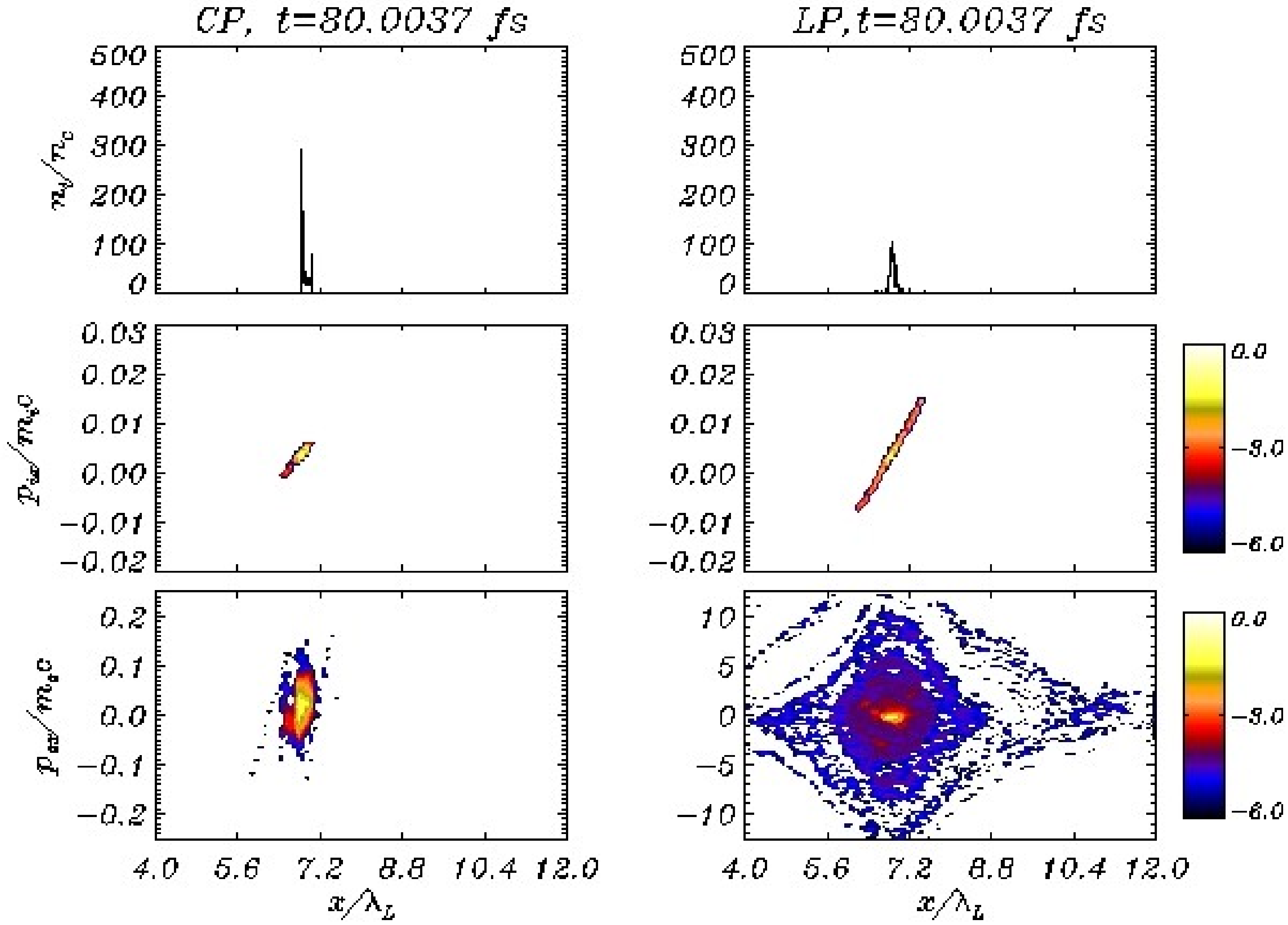

CP: Electrons are “cold” (~keV)
Foil accelerated as a whole

LP: Electrons are “hot” (~MeV)
foil explodes, broad ion spectrum

Simulation of thin foil acceleration: CP vs. LP

- Carbon target, thickness d=0.04μ m, n_e=250n_c=4.3×10^{23} cm^{-3}
- Laser: 26 fs pulse, I=1.8×10^{20} W/cm^2

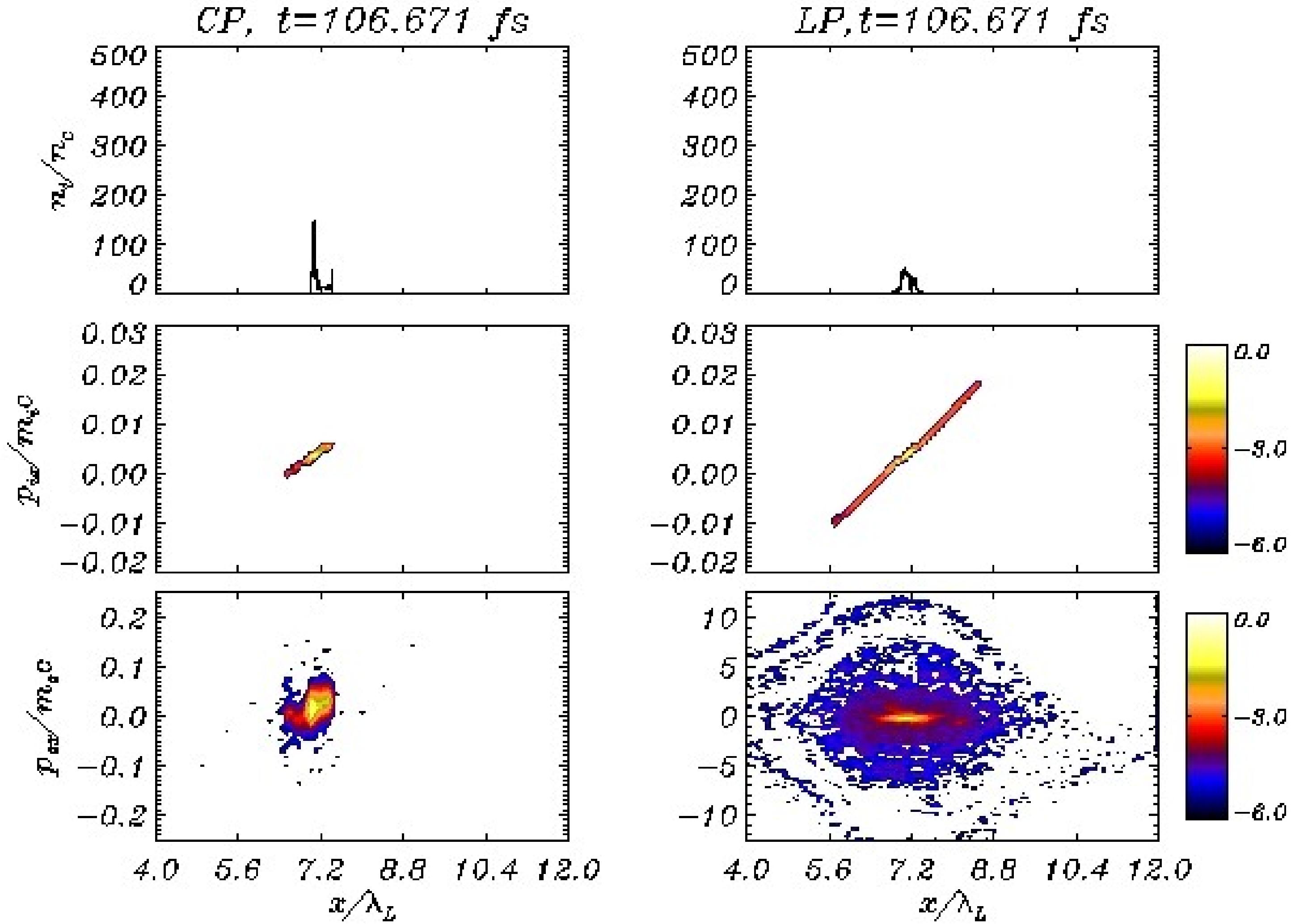

CP: Electrons are "cold" (~keV)
Foil accelerated as a whole

LP: Electrons are "hot" (~MeV)
foil explodes, broad ion spectrum

Simulation of thin foil acceleration: CP vs. LP

- Carbon target, thickness d=0.04μ m, n_e=250n_c=4.3×10^{23} cm^{-3}
- Laser: 26 fs pulse, I=1.8×10^{20} W/cm^{2}

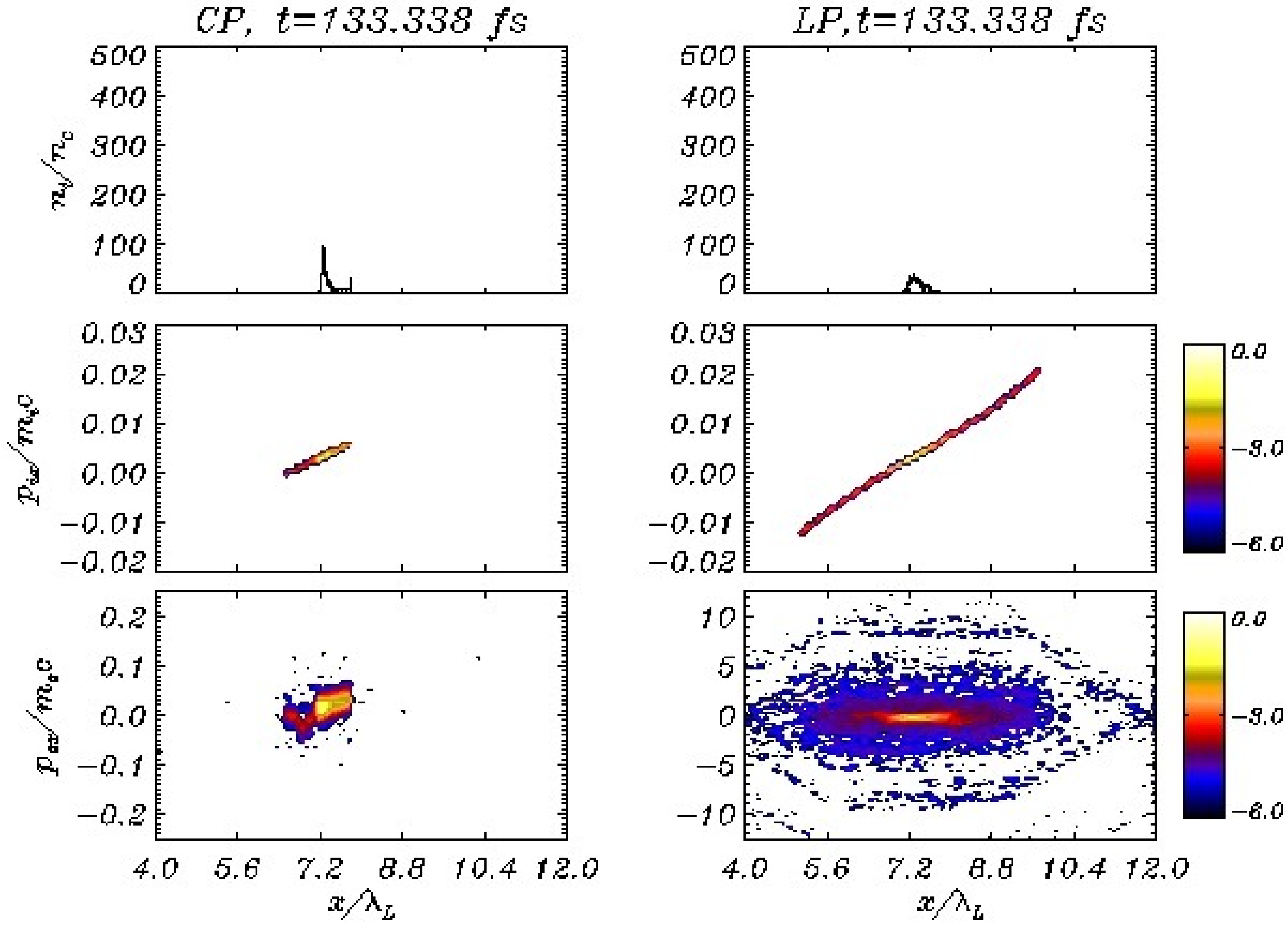

CP: Electrons are "cold" (~keV)
Foil accelerated as a whole

LP: Electrons are "hot" (~MeV)
foil explodes, broad ion spectrum

Simulation of thin foil acceleration: CP vs. LP

- Carbon target, thickness d=0.04μ m, n_e=250n_c=4.3×10^{23} cm^{-3}
- Laser: 26 fs pulse, I=1.8×10^{20} W/cm^2

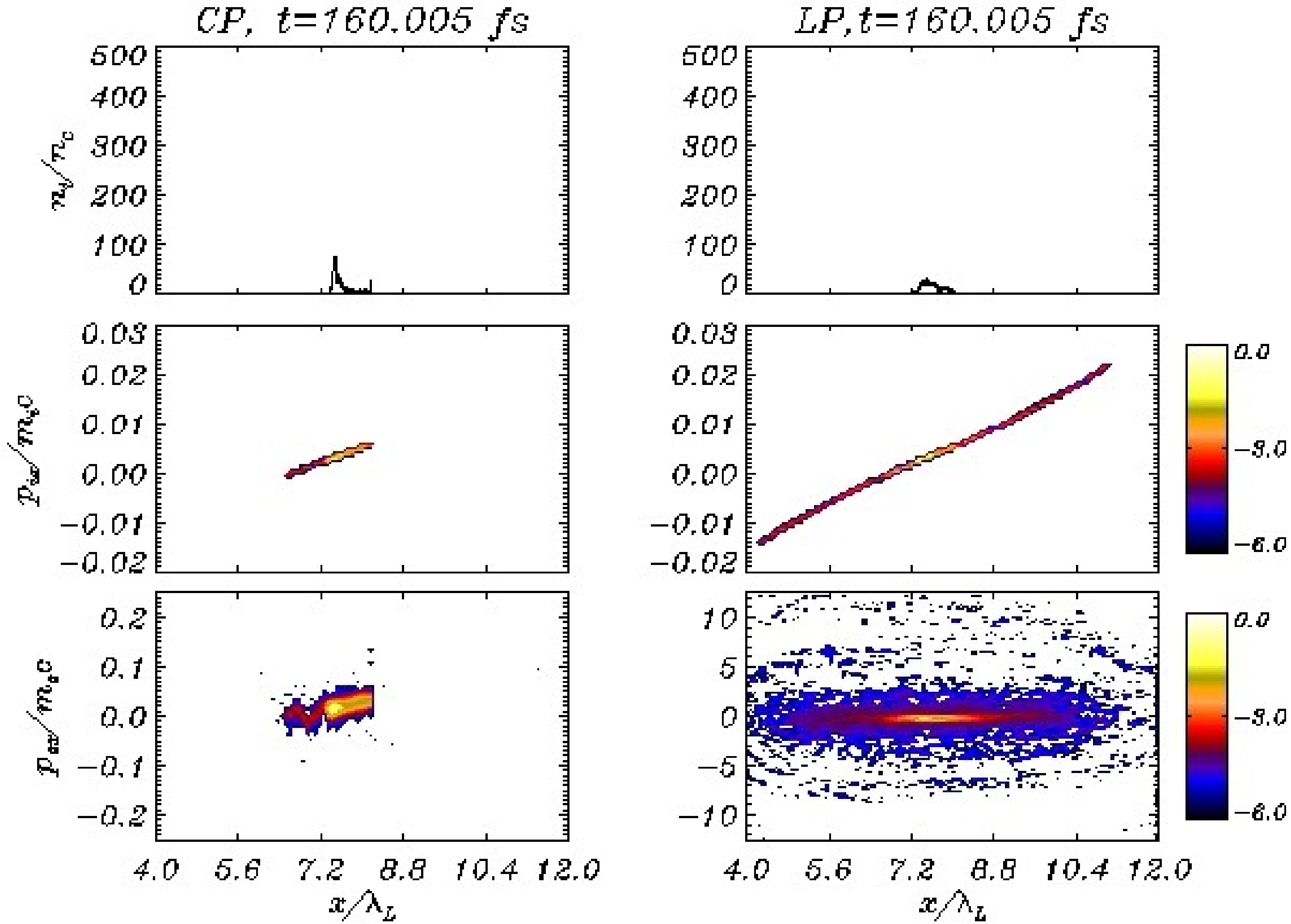

CP: Electrons are “cold” (~keV)
Foil accelerated as a whole

LP: Electrons are “hot” (~MeV)
foil explodes, broad ion spectrum

“Optimal” thickness for thin foil RPA

For the foil to be accelerated as a whole, the thickness ℓ must match the laser penetration depth d_p

$\ell >> d_p$: the foil is accelerated “by slices”

[A.Macchi et al, PRL **94**, 165003 (2005)]

$\ell << d_p$: all electrons are blown away: Coulomb explosion of the foil

the thinner the foil:

- the lower the mass and the higher the final velocity and energy per nucleon
- the lower the reflectivity R and the radiation pressure in the rest frame $P_{\mathrm{rad}}=(2I/c)R$

An “optimal” compromise can be reached for nm-thick foils (technologically feasible!)

Model for nonlinear "relativistic" reflectivity

Ultrathin slab model: $n_e(x)=n_0\ell\delta(x)$, foil thickness $\ell<<\lambda$

Nonlinear reflectivity $R=R(\zeta,a_0)$ can be computed analytically

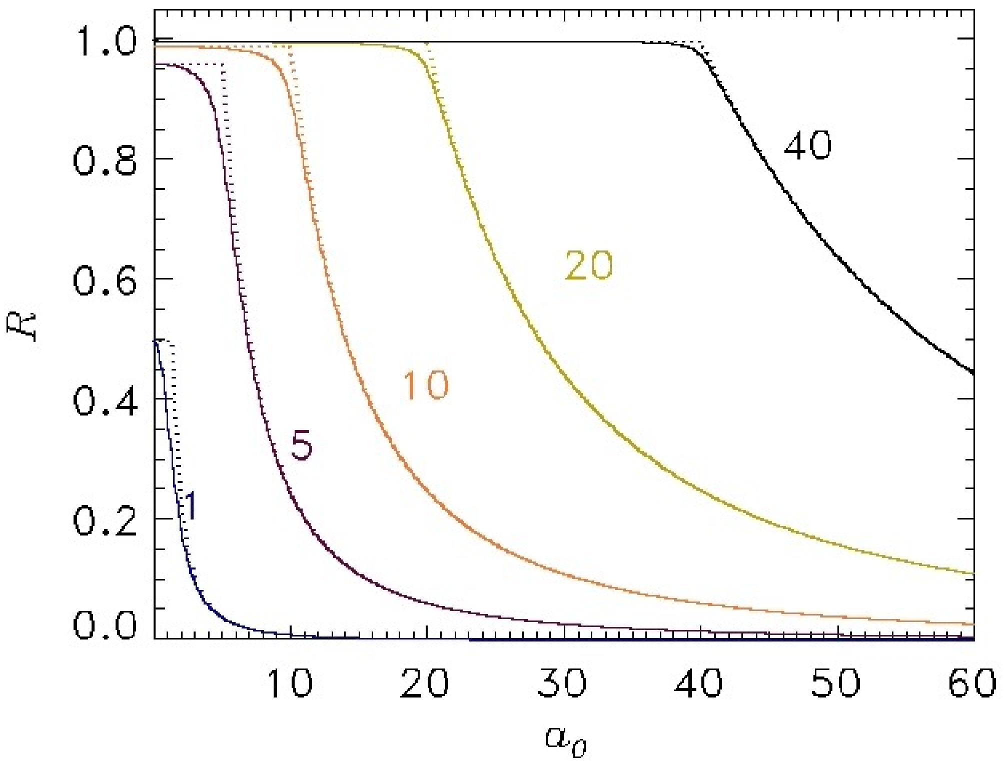

approximated (but rather precise) formula:

$R\approx\zeta^2/(\zeta^2+1)$ for $a_0<\zeta$

$R\approx\zeta^2/a_0^2$ for $a_0>\zeta$

$P_{rad}=(2I/c)R$ does ***not*** depend on a_0 for $a_0>\zeta$! (since $I\sim a_0^2$)

The maximum boost of the foil is at $a_0\approx\zeta$

[A.Macchi, S. Veghini, F. Pegoraro, PRL **103**, 085003 (2009)]

Comparison of LS model with 1D PIC simulations

Laser pulse: a_0=**5-50**, τ=8 cycles ("flat-top" envelope)

Thin foil target: $n_e=250n_c$, ℓ=**0.01-0.1λ** (ζ=**7.8-78.5**)

Energy spectra vs. a_0 and ℓ:

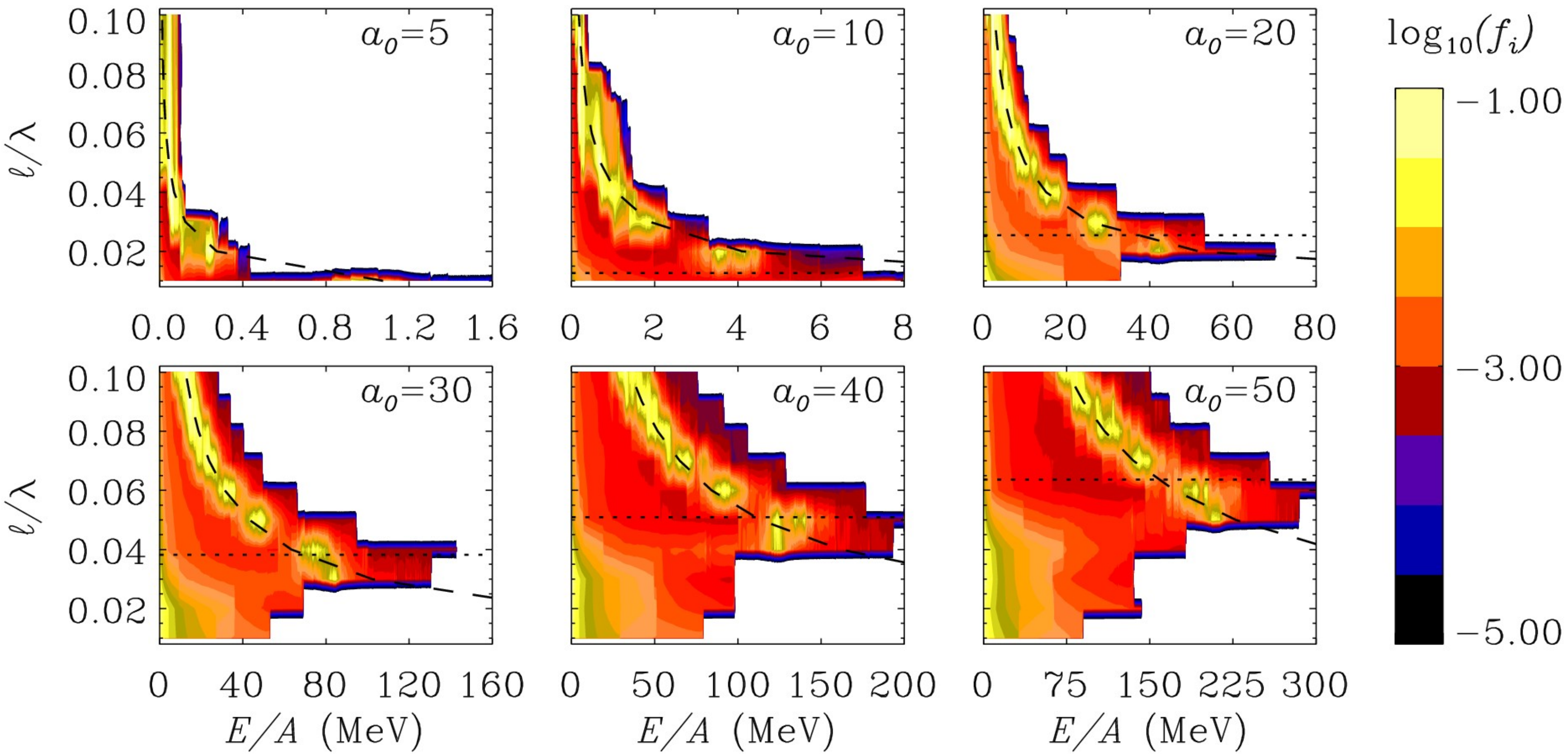

[A.Macchi, S. Veghini, F. Pegoraro, PRL **103**, 085003 (2009)]

Comparison of LS model with 1D PIC simulations

Laser pulse: a_0=**5-50**, τ=8 cycles (“flat-top” envelope)

Thin foil target: n_e=250n_c , ℓ=**0.01-0.1**λ (ζ=**7.8-78.5**)

Energy spectra vs. a_0 and ℓ:

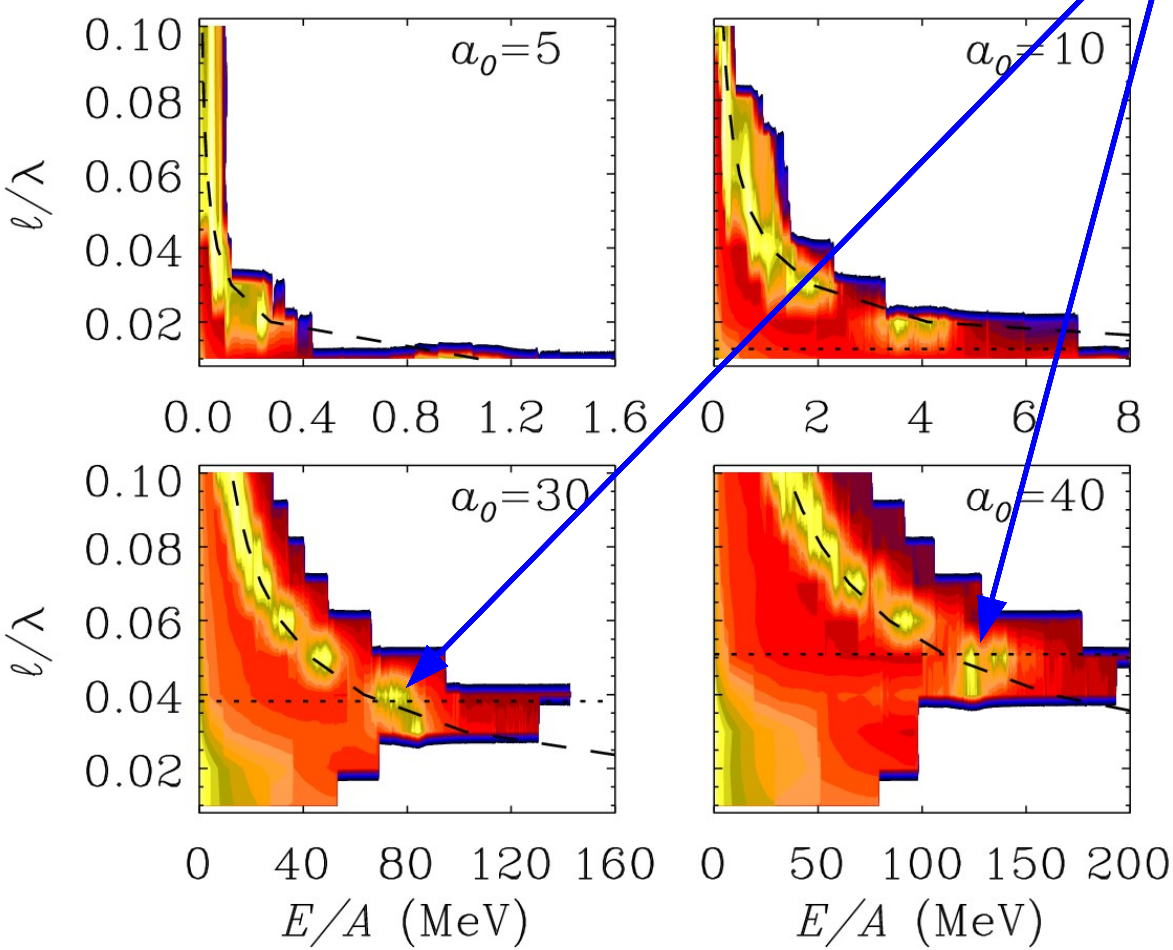

A **narrow spectral peak** is observed for $a_0 < \zeta$. The max energy is at $a_0 = \zeta$ (dotted line)

The energy of the peak is in good agreement with the LS formula (dashed black line)

[A.Macchi, S. Veghini, F. Pegoraro, PRL **103**, 085003 (2009)]

Comparison of LS model with 1D PIC simulations

Laser pulse: a_0=**5-50**, τ=8 cycles ("flat-top" envelope)

Thin foil target: $n_e = 250 n_c$, ℓ=**0.01-0.1**λ (ζ=**7.8-78.5**)

Energy spectra vs. a_0 and ℓ:

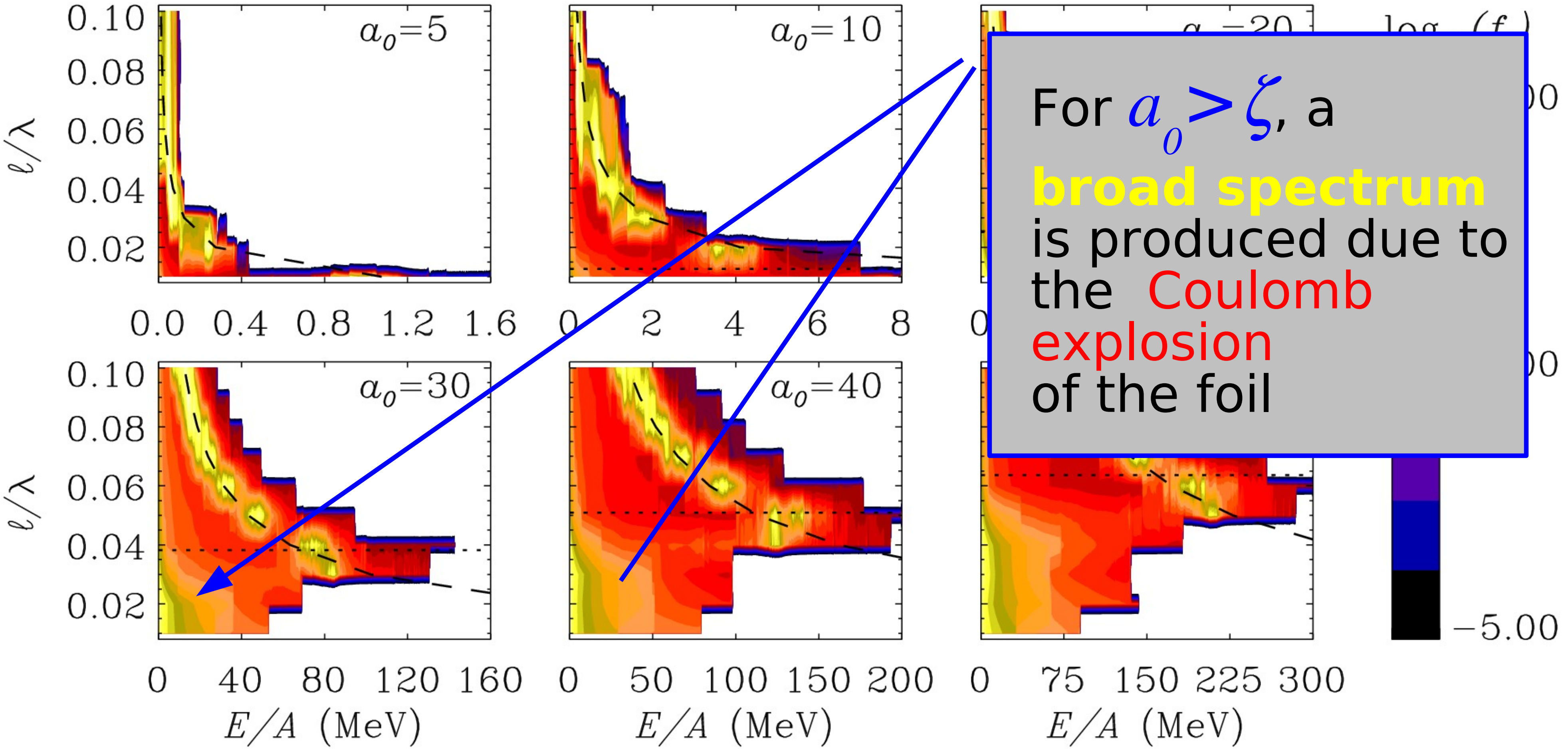

[A.Macchi, S. Veghini, F. Pegoraro, PRL **103**, 085003 (2009)]

Comparison of LS model with 1D PIC simulations

Laser pulse: a_0=**2.9-29**, τ=9 cycles ("sin^2" envelope)

Thin foil target: n_e=250n_c, ℓ=**0.005-0.06**λ

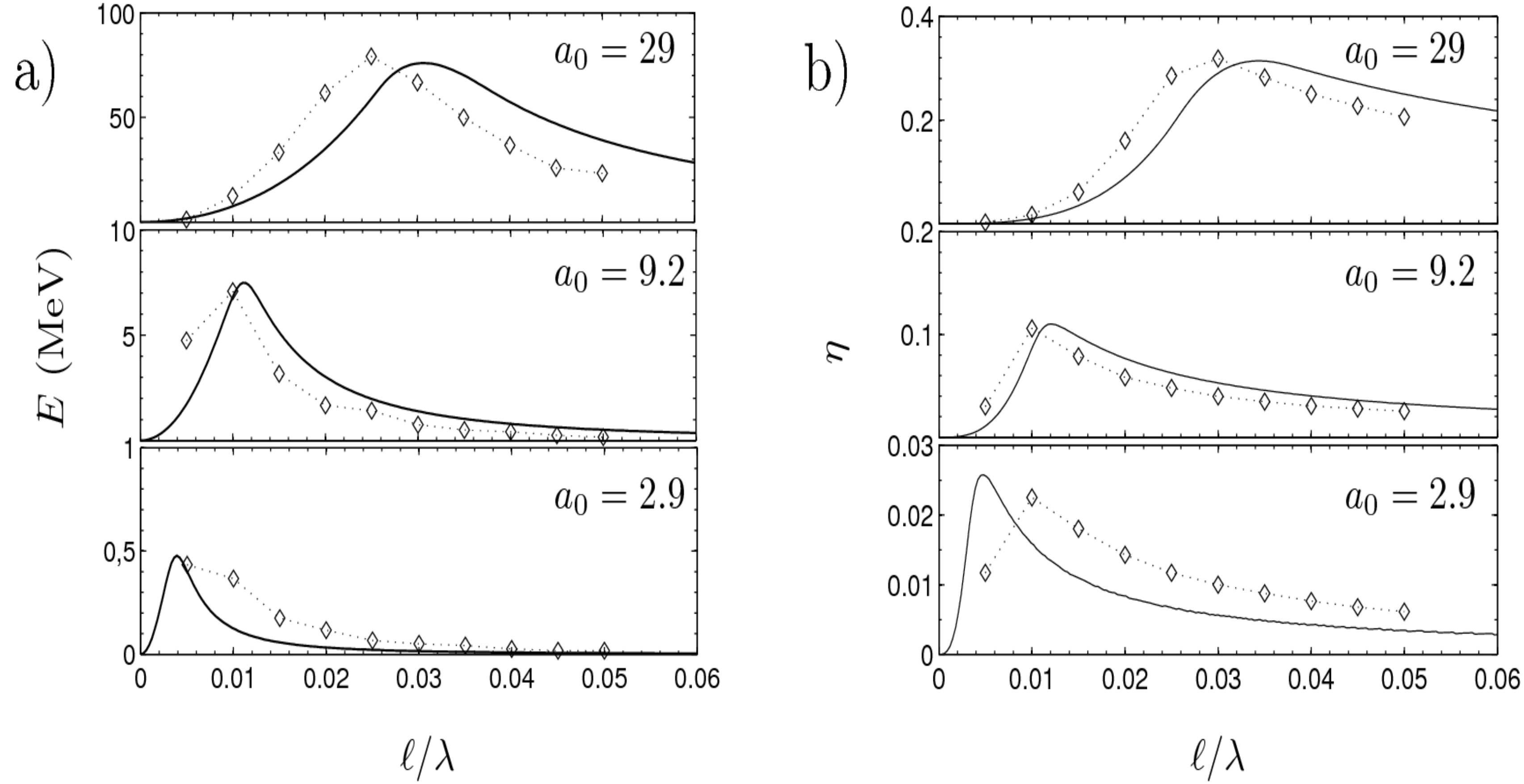

The energy of the peak and the conversion efficiency are in good agreement with the LS model modified to account for nonlinear reflectivity effects

[A.Macchi, T. Lyseikina, S. Veghini, F. Pegoraro, New. J. Phys (2010)]

A rich dynamics beneath the simple LS model...

- The foil is not "rigid": the radiation pressure separates electrons from ions, charge separation effects are dominant

- self-organization of electrons and ions keep electrostatic and radiation pressures in equilibrium and ensure "stable" acceleration in a suitable parameter range

- 3D simulations confirm 1D scenario, while accounting for the additional constraint of Conservation of the Angular Momentum carried by the CP pulse

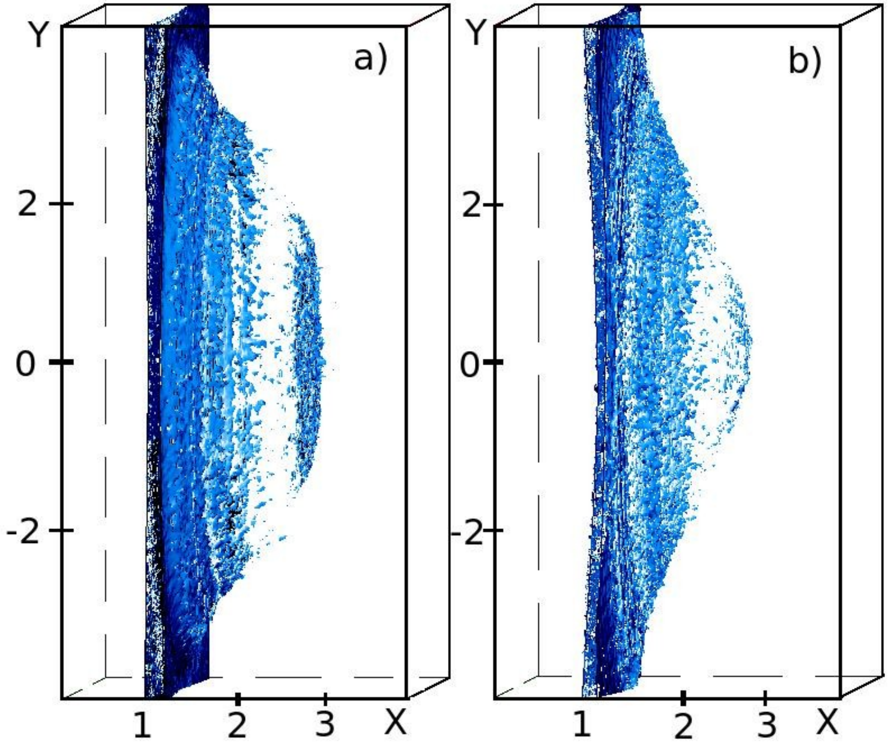

For details and further reading:

T.V.Liseikina et al,
Plasma Phys. Contr. Fus. **50** ,
124033 (2008)

A.Macchi et al, PRL **103**, 085003
(2009)

A.Macchi et al, New.J.Phys., in press

and (many) references therein

First experimental indications of CP-RPA

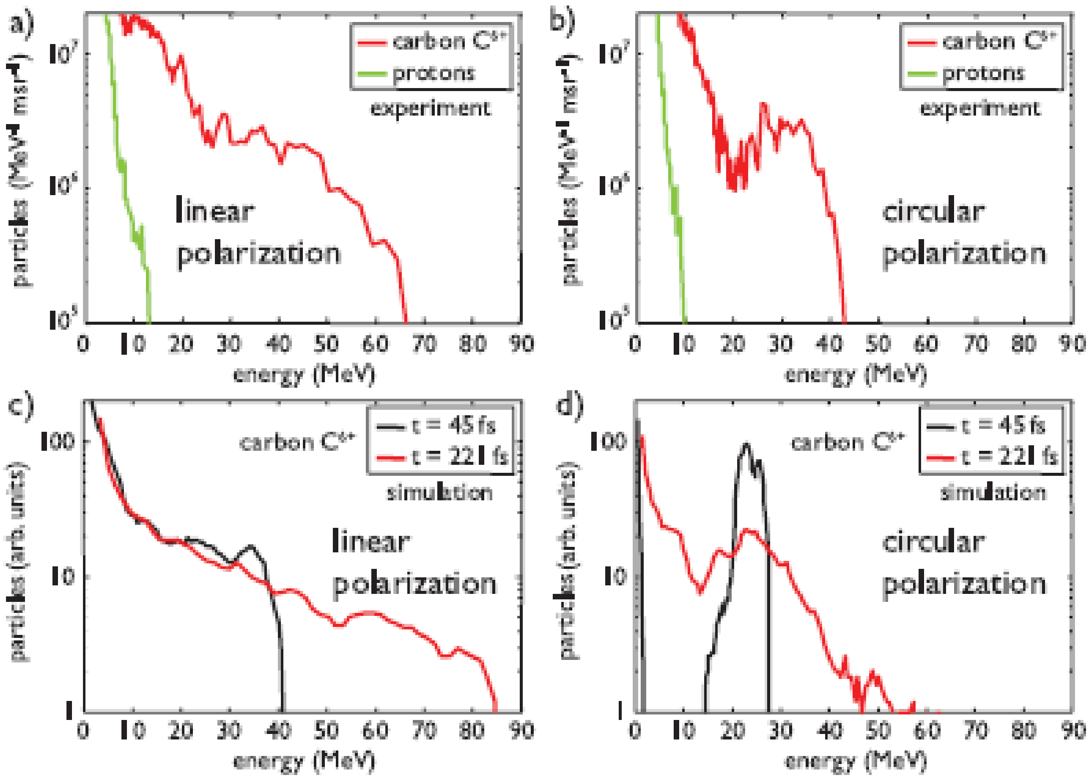

FIG. 2 (color). Experimentally observed proton (green curves) and carbon C^{6+} (red curves) spectra in the case of linear (a) and circular (b) polarized irradiation of a 5.3 nm thickness DLC foil. The corresponding curves as obtained from 2D PIC simulations (c),(d) show excellent agreement with the measured distributions at late times (red curves, $t = 221$ fs after the arrival of the laser pulse maximum at the target). A quasimonoenergetic peak generated by radiation-pressure acceleration is revealed for circular polarization, being still isolated at the end of the laser-target interaction (black curve, $t = 45$ fs).

A.Henig et al,
PRL **103** (2009) 245003
(MBI Berlin)

laser pulse:
45 fs, $I=5\times10^{19}$ W/cm^2

target:
Diamond-Like Carbon
ultrathin foils (3-10 nm)

Similar results obtained by LIBRA collaboration with GEMINI @ RAL, UK

(M.Borghesi,
talk at COULOMB09,
Senigallia, Italy,
June 2009)

Conclusions

- Most experiments on ion (proton) acceleration from solid targets reported so far are well explained by the TNSA mechanism

- The plasma expansion model gives a fair description of energy scaling (but needs the input of “unknown” parameters...)

- TNSA offers a reliable framework for ion source development and optimization (target engineering, dynamic beam control)

- Scaling of TNSA at higher intensities and suitability for foreseen applications (fusion, hadrontherapy) is an open issue

- RPA of ultrathin targets is attractive due to favorable scalings, high efficiency and monoenergeticity

- The Light Sail model offers a simple but effective description of RPA

- Experimental investigations of RPA with CP pulses are in progress

This talk may be downloaded from

www.df.unipi.it/~macchi/talks.html

Basis of theoretical and numerical modeling

"Plasma physics is just waiting for bigger computers"

Vlasov-Maxwell system for *collisionless, classical* plasmas: kinetic equations are coupled to EM fields

$$\frac{df_a}{dt}(\mathbf{x},\mathbf{p},t) = \frac{\partial f_a}{\partial t} + \dot{\mathbf{x}}_a \frac{\partial f_a}{\partial \mathbf{x}} + \dot{\mathbf{p}}_a \frac{\partial f_a}{\partial \mathbf{p}} = 0, \quad a = (e,i)$$

$$\dot{\mathbf{p}}_a = q_a(\mathbf{E} + \mathbf{v} \times \mathbf{B}), \qquad \dot{\mathbf{x}}_a = \frac{\mathbf{p}_a}{m_a \gamma_a},$$

$$\rho(\mathbf{x},t) = \sum_{a=e,i} q_a \int d^3p f_a, \qquad \mathbf{J}(\mathbf{x},t) = \sum_{a=e,i} q_a \int d^3p \mathbf{v} f_a,$$

$$\nabla \cdot \mathbf{E} = \rho, \qquad \nabla \cdot \mathbf{B} = 0, \qquad \nabla \times \mathbf{E} = -\partial_t \mathbf{B}, \qquad \nabla \times \mathbf{B} = \mathbf{J} + \partial_t \mathbf{E}$$

Mostly used numerical approach: particle-in-cell (PIC) method
[Birdsall & Langdon, *Plasma Physics via Computer Simulation* (IOP, 1991)]

3D numerical simulations of "realistic" experimental conditions is most of the times beyond present-day supercomputing power

Models are needed to interpretate experiments and unfold the underlying physics